The Effect of Counterion/Ligand Interplay on the Activity and Stereoselectivity of Palladium(II)–Diimine Catalysts for CO/*p*-Methylstyrene Copolymerization

Barbara Binotti,[b] Gianfranco Bellachioma,[a] Giuseppe Cardaci,[a] Carla Carfagna,[b] Cristiano Zuccaccia,[a] and Alceo Macchioni*[a]

Abstract: The catalytic activity and stereoselectivity of complexes $[Pd(\eta^1,\eta^2-C_8H_{12}OMe)(Ar-N=C(R')-C(R')=N-Ar)]X$ in the copolymerization of CO and *p*-methylstyrene have been correlated with their interionic structure in solution and in the solid state, as determined by $^{19}F,^1H$-HOESY NMR spectroscopy and X-ray diffraction studies, respectively. The highest productivity is obtained with unhindered diimine ligands bearing electron-donating substituents and with the least coordinating counterion. Copolymers with a microstructure ranging from atactic to predominantly isotactic are obtained. The degree of isotacticity increases as the steric hindrance in the apical positions and the coordinating ability of the counterion increase. The counterion is located close to the diimine in both solution and the solid state but it moves toward the palladium as the steric hindrance in the apical positions decreases. When the latter is small the counterion competes with the substrate for apical coordination, and consequently it affects the productivity. In the case of *ortho*-dimethyl-substituted ligands the counterion is confined in the back, above the $N=C(R')-C(R')=N$ moiety, and does not affect the productivity. However, it contributes to increasing the stereoregularity of the copolymer by making the aryl moieties more rigid. With $R'=Me$ and $Ar=o-Me_2C_6H_3$ an *ll* of 81% and 72% was obtained with $X^-=CF_3SO_3^-$ or $BArF^-$, respectively. The isotacticity of the copolymers produced by *ortho*-monosubstituted catalysts depends greatly on the counterion and ranges from 30% to 59% with $X^-=BArF^-$ and $X^-=CF_3SO_3^-$, respectively, with $Ar=o-EtC_6H_4$ and $R'=Me$. Based on the interionic structural results, this effect can be explained by a greater reduction of the copolymerization rate of C_s-symmetric isomers with respect to their C_2-symmetric counterparts.

Keywords: copolymerization · ion pairs · N ligands · NMR spectroscopy · palladium

Introduction

Homogeneous polymerization of olefins[1–4] and carbon monoxide/olefin copolymerizations[5–7] are currently catalyzed by metal-organic ion pairs of general formula $[L_nM-R]^+\cdots X^-$. Extensive studies have shown that the interplay between the counterion and the cationic moiety significantly affects the catalytic performance and, consequently, the microstructure of the resulting polymeric materials. This is particularly true for the polymerization of olefins catalyzed by organometallic complexes of early transition metals that are usually carried out in low polar solvents such as benzene, toluene, or isoparaffins.[8–10] The counterion effects are less marked in CO/olefin copolymerization[6,10–16] and even less so in the polymerization of olefins catalyzed by late transition metal organometallic complexes,[17] partly because they are often performed in moderate (dichloromethane) to highly (methanol) polar solvents.

Among the numerous complexes capable of catalyzing polymerization reactions, palladium(II) complexes bearing *ortho*-substituted aryl diimines [Ar−N=C(R′)−C(R′)=N−Ar] are rather peculiar as, depending on the steric hindrance of the *ortho* substituents, they are excellent catalysts for polymerization[18,19] of olefins or reasonably good catalysts for

[a] Prof. G. Bellachioma, Prof. G. Cardaci, Dr. C. Zuccaccia,
Prof. A. Macchioni
Dipartimento di Chimica, Università di Perugia
Via Elce di Sotto, 8-06123 Perugia (Italy)
Fax: (+39) 075-585-5598
E-mail: alceo@unipg.it

[b] Dr. B. Binotti, Dr. C. Carfagna
Istituto di Scienze Chimiche "F. Bruner"
Università di Urbino "Carlo Bo"
Piazza Rinascimento, 6-61029 Urbino (Italy)

the alternating copolymerization of CO and aromatic olefins.[20,21] The key to switching the catalytic activity from olefin polymerization to CO/olefin copolymerization is to introduce steric bulk in the apical positions by way of the *ortho* substituents. When these substituents are large the catalysts are ideal for the polymerization of olefins and produce high-molecular-weight hyperbranched polymers;[22] when they are small the catalysts afford CO/olefin copolymers.[20,23] In the former case, it is beneficial that the apical position is not accessible to the olefin to minimize the termination processes that can occur by chain transfer,[24,25] whereas in the latter case the apical positions have to be accessible to the monomers or to the carbonyl moiety of the last inserted CO in order for the copolymerization to proceed.[26,27] The steric hindrance in the apical positions can also be indirectly modulated by changing the substituents in the back.[28,29] In particular, a reduction of the size of R′ allows the aryl moiety to oscillate, with a consequent relief of apical encumbrance. Finally, another source of apical hindrance is the counterion, which in square-planar complexes prefers to be located above and below the coordination plane and shifted toward the diimine ligands.[13,30–32] This means that there is a sort of competition between the counterion and the *ortho* substituents to occupy the apical positions. Interionic NOE NMR studies have indicated that the counterion can access the metal center only when the *ortho* substituents are smaller than methyl groups.[23] This could explain why the counterion has a greater effect on the catalytic activity of CO/olefin copolymerization, where small *ortho* substituents are used, than on the polymerization of olefins, where large *ortho* substituents are necessary.

All these considerations seem to indicate that an ideal cationic catalyst for the CO/olefin copolymerization should possess *ortho* and R′ substituents that introduce the smallest encumbrance in the apical positions and be compensated by the least coordinating counterion. This is true as far as the catalytic activity is concerned but it is not always true for the stereoregularity of the copolymers. As a confirmation, we have previously communicated[20] that the use of *ortho*-dimethyl-substituted diimines instead of *ortho*-unsubstituted ones not only leads to a decrease in the catalytic activity but also to a substantial increase in the isotacticity of the copolymer, which also depends slightly on the nature of the counterion.
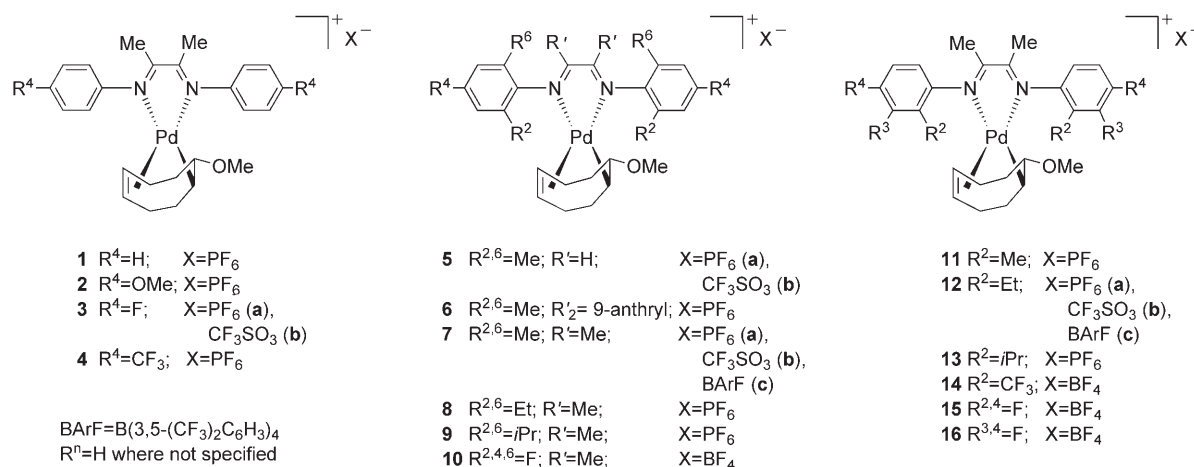
We report here in full the delicate interplay between the steric features of the aryl diimine ligands and the counterion in determining the activity and stereoselectivity of the palladium(II) catalysts shown below. The steric hindrance in the apical positions is varied by changing the substituents R^2, R^4, R^6, and R′ (complexes **1–10**). The electronic features of the diimine ligands are also varied in complexes **1–4** by changing the R^4 substituents leaving, in some cases, the steric hindrance in the apical positions unaltered. Finally, Pd catalysts bearing *ortho*-monosubstituted aryl diimines (**11–16**) have been investigated since the ligand/counterion interplay for such complexes may be more critical because it alters the symmetry of the catalytic center (vide infra). The main aim of the paper is to correlate the interionic structure of the catalysts, as determined in solution by low-temperature $^{19}F,^{1}H$-HOESY NMR studies and in the solid state by X-ray single-crystal diffractometry, with their activity and stereoselectivity.
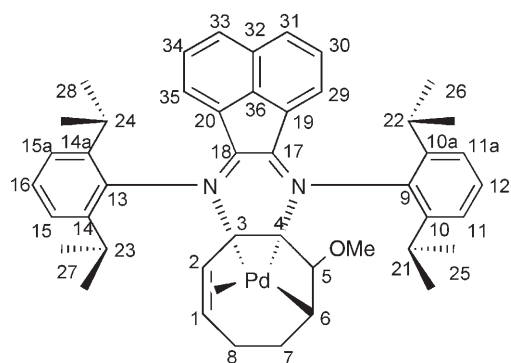
Results

Synthesis and characterization of Pd complexes in solution: The palladium(II) complexes were synthesized by treatment of the dimer $[Pd(\eta^1,\eta^2\text{-}C_8H_{12}OMe)Cl]_2$ with two equivalents of the appropriate nitrogen ligand either in methanol in the presence of NH_4PF_6 (**1**, **2**, **3a**, **4**, **5a**, **6**, **7a**, **8**, **9**, **11**, **12a**, and **13**) or in dichloromethane in the presence of the appropriate silver or sodium salt (**3b**, **5b**, **7b**, **7c**, **10**, **12b**, **12c**, **14**, **15**, and **16**).

Their structure was investigated in CD_2Cl_2 by ^{1}H, ^{13}C, ^{19}F, and ^{31}P NMR spectroscopy. The assignment of the ^{1}H, ^{13}C, and ^{19}F resonances was performed by following the scalar and dipolar nuclear interactions in the ^{1}H-COSY, ^{19}F-COSY, $^{1}H,^{13}C$-HMQC, $^{1}H,^{13}C$-HMBC, ^{1}H-NOESY, ^{19}F-NOESY, and $^{19}F,^{1}H$-HOESY spectra. Data are reported in the Exper-

1 R^4=H; X=PF$_6$
2 R^4=OMe; X=PF$_6$
3 R^4=F; X=PF$_6$ (**a**), CF$_3$SO$_3$ (**b**)
4 R^4=CF$_3$; X=PF$_6$

BArF=B(3,5-(CF$_3$)$_2$C$_6$H$_3$)$_4$
R^n=H where not specified

5 R^{2,6}=Me; R′=H; X=PF$_6$ (**a**), CF$_3$SO$_3$ (**b**)
6 R^{2,6}=Me; R′$_2$= 9-anthryl; X=PF$_6$
7 R^{2,6}=Me; R′=Me; X=PF$_6$ (**a**), CF$_3$SO$_3$ (**b**), BArF (**c**)
8 R^{2,6}=Et; R′=Me; X=PF$_6$
9 R^{2,6}=iPr; R′=Me; X=PF$_6$
10 R^{2,4,6}=F; R′=Me; X=BF$_4$

11 R^2=Me; X=PF$_6$
12 R^2=Et; X=PF$_6$ (**a**), CF$_3$SO$_3$ (**b**), BArF (**c**)
13 R^2=iPr; X=PF$_6$
14 R^2=CF$_3$; X=BF$_4$
15 R^{2,4}=F; X=BF$_4$
16 R^{3,4}=F; X=BF$_4$

Scheme 1.

imental Section. C5 (see Scheme 1 for numbering) of the methoxycyclooctenyl moiety was the starting point for the assignment since it resonates at about $\delta = 80$ ppm, which is rather distant from all the other signals.

A dynamic process that exchanges the two N-arms of the α-diimine ligands is present for all the complexes. Its rate increases on decreasing the steric hindrance and on increasing the number of electron-withdrawing substituents on the ligand.[23] Fortunately, as the temperature is decreased the exchange process becomes slower with respect to both the chemical-shift and relaxation timescale for almost all the complexes. The only exceptions are the complexes with unhindered diimine ligands having several electron-withdrawing substituents. For example, exchange cross-peaks are observed in the ^{19}F-NOESY NMR spectrum of complex **10** (CD$_2$Cl$_2$, 199 K) between F14a and F10 and F10a and F14 (Scheme 1), thus indicating that the fluxional motion is slow on the chemical-shift timescale but fast on the longitudinal-relaxation timescale, even at this temperature. In this case it was not possible to discriminate the resonances of the two sides of the diimine ligand.

The NMR spectra of the *ortho*-monosubstituted compounds **11–16** show broad resonances at room temperature that split into complicated sets of sharp resonances upon
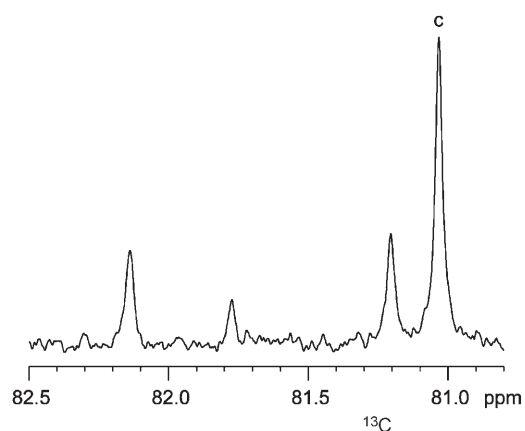

Figure 1. Section of the ^{13}C NMR spectrum (100.61 MHz, 217 K, CD$_2$Cl$_2$) of complex **12a** showing the C5 resonances of the four isomers.

lowering the temperature (Figure 1). The latter are due to the simultaneous presence of all four possible conformational isomers in which the relative orientations of the R^2 substituents differ with respect to the square coordination plane (Scheme 2). The nitrogen ligand adopts a C_2- (*a* and *b* in Scheme 2) or a C_s-symmetric coordination geometry (*c* and *d*, Scheme 2).
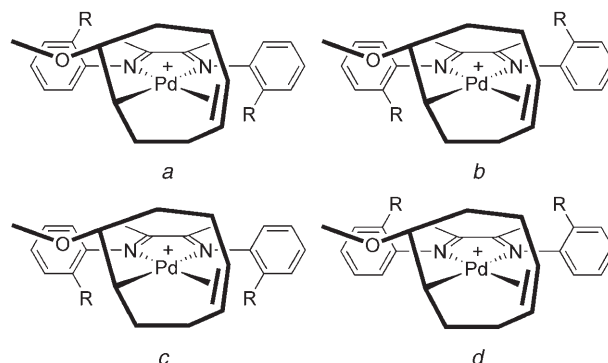
Scheme 2.

^{1}H-NOESY NMR investigations allowed the prevalent isomer *c* for complexes **11–13** and the second most abundant isomer *d* for complex **14** to be assigned. For example, strong H5/H10a and H2/H14a contacts are observed in the ^{1}H-NOESY NMR spectrum of complex **12a** (Figure 2) for the prevalent isomer, in strict agreement with the orientation of both the *ortho*-ethyl substituents on the opposite side with respect to the OMe group.

The most abundant isomer in complex **14** (R^2=CF$_3$) could not be identified by ^{1}H-NOESY studies due to the overlapping of the H1 and H2 resonances. Despite this, the observation of strong interionic contacts between BF$_4$$^-$ and both H10a and H14a, and the absence of any interionic interactions in the ^{19}F-NOESY NMR spectrum (vide infra), strongly suggest that *c* is also the major isomer in this case. ^{19}F,^{1}H-HOESY NMR investigations also indicated that isomer *d* is the second most abundant one in complex **14**. The above-mentioned dynamic process is also fast on the relaxation timescale at the minimum possible temperature for **15** and **16**, which prevented the assignment of the most abundant isomer(s).

The relative percentage of the predominant isomer *c*[33] for complexes **11** (R^2=Me), **12a** (R^2=Et), **13** (R^2=*i*Pr), and **14** (R^2=CF$_3$) was determined to be 52, 58, 64, and 59%, respectively. This percentage depends on the counterion, and is 46% in **12c** (R^2=Et, X=BArF), 58% in **12a** (R^2=Et, X=PF$_6$), and 56% in **12b** (R^2=Et, X=CF$_3$SO$_3$).

Crystals of the *c* isomer of complex **13** (R^2=*i*Pr, X=PF$_6$; vide infra) were dissolved in CD$_2$Cl$_2$ at 217 K in an NMR tube to give a solution containing 91% of isomer *c* at equilibrium. Upon warming the solution to room temperature an interconversion process between the isomers occurred that led to thermodynamic equilibrium mixtures of all four conformers within several hours.
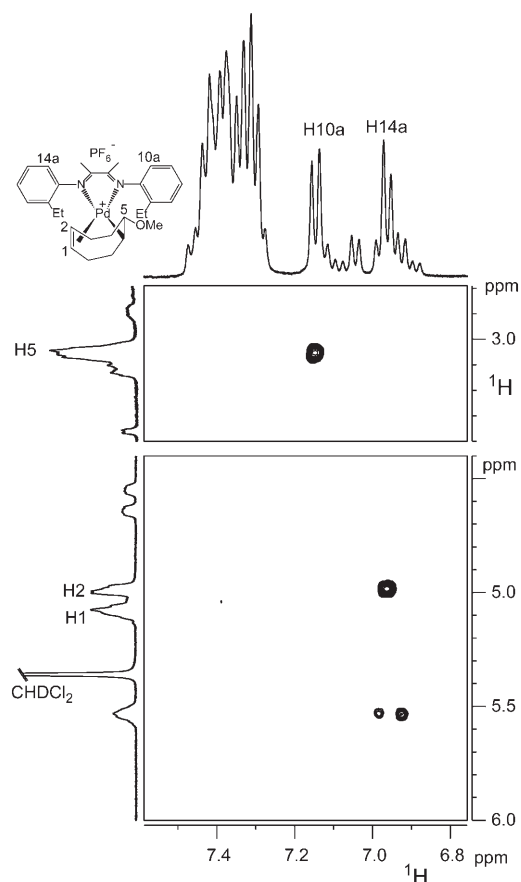
Figure 2. Two sections of the ^{1}H-NOESY NMR spectrum (400.13 MHz, 217 K, CD$_2$Cl$_2$) of complex **12a** showing the specific contacts of H5 with H10a and H2 with H14a.

The solution interionic structure of **1**–**16** was investigated in CD$_2$Cl$_2$ by ^{19}F,^{1}H-HOESY and ^{19}F-NOESY NMR spectroscopy. In all cases the anion is located close to the electropositive diimine carbons,[32] although its exact position is finely modulated by the steric hindrance of the R^2 and R^6 substituents. The counteranion interacts with H5, H1, and H2 of the 5-methoxycyclooctenyl moiety only when R^2 = R^6 = H (complexes **1**–**4**; Figure 3), while in the *ortho*-disubstituted complexes **5**–**10** it interacts exclusively with the protons of the diimine ligands.

In the predominant *c* isomer of *ortho*-monosubstituted compounds **11**–**16** the anion shows very strong interactions with H10a and H14a, while those with the protons of R^2 are almost absent (Figure 4). This indicates that the counterion approaches the cation from the nonhindered side of the N,N ligand. As a confirmation, anion/CF$_3$ interactions are absent from the ^{19}F-NOESY NMR spectrum of complex **14**. Selective interactions were also detected between the anion and protons H2 and H5 of the methoxycyclooctenyl moiety (Figure 4).

Interionic structure in the solid state: The structures of **3a**, **5a**, **7a**, and **13** were determined by X-ray single crystal diffractometry. They do not show any particular feature from
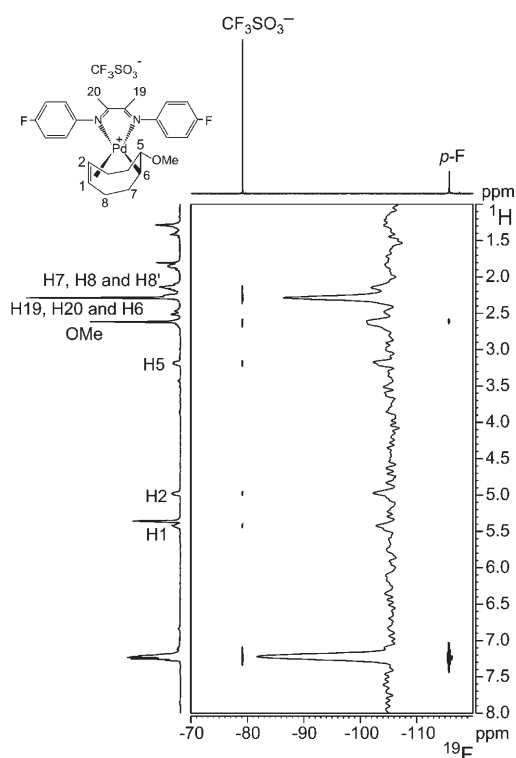

Figure 3. ^{19}F,^{1}H-HOESY NMR spectrum (376.63 MHz, 273 K, CD$_2$Cl$_2$) of complex **3b**. CF$_3$SO$_3^-$ interacts with most of the proton resonances. The internal projection is relative to the CF$_3$SO$_3^-$ column.

an intramolecular point of view with respect to the structures of related compounds.[13,25,34–40] Some disorder was observed for the methoxycyclooctenyl moiety for compounds **3a**, **5a**, and **7a**, although this does not prevent us from obtaining crucial information regarding the interionic structure.

In all cases the closest PF$_6^-$ counterion was found above the diimine carbons of the *N,N*-ligand [C(17) and C(18)]. Its actual position depends critically on the steric hindrance of the aryl *ortho* substituents and on the backbone group (Figure 5). The relative position of the anion can be conveniently described by the vertical distance of the P atom of the anion from the Pd-N(1)-C(17)-C(18)-N(2) mean plane and from the horizontal distance between the Pd atom and the intercept of the vertical distance (Figure 5). The latter distance is much shorter for complexes having H (**3a**: 2.115 Å; **13**: 2.378 Å) instead of Me (**7a**: 4.723 Å; **5a**: 5.480 Å) substituents at the *ortho* positions (Figure 5). The vertical distance is roughly the same for **3a** (4.025 Å), **13** (4.134 Å), and **7a** (3.994 Å), while it is considerably smaller for **5a** (2.982 Å).

CO/*p*-methylstyrene copolymerization: The synthesized α-diiminepalladium(II) complexes were tested in the copolymerization of CO and *p*-methylstyrene in dichloromethane at room temperature and 1 atm of carbon monoxide (Table 1).
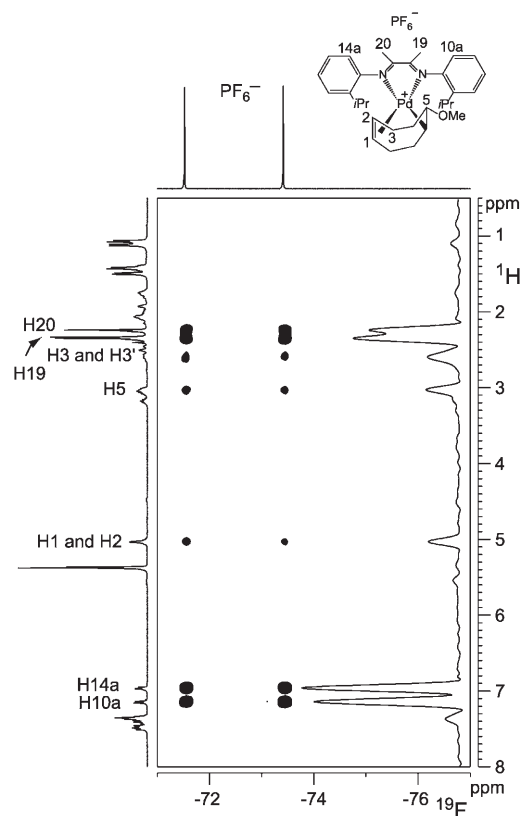
Figure 4. ^{19}F,^{1}H-HOESY NMR spectrum (376.63 MHz, 217 K, CD$_2$Cl$_2$) of complex **13**. The PF$_6^-$ interacts preferentially with the backbone methyl groups (H19 and H20) and with H10a and H14a. Note the small, selective interactions of the anion with H2 and H5 methoxycyclooctenyl moiety for the major isomer. The F1 trace (indirect dimension) of one component of the fluorine doublet is shown on the right.
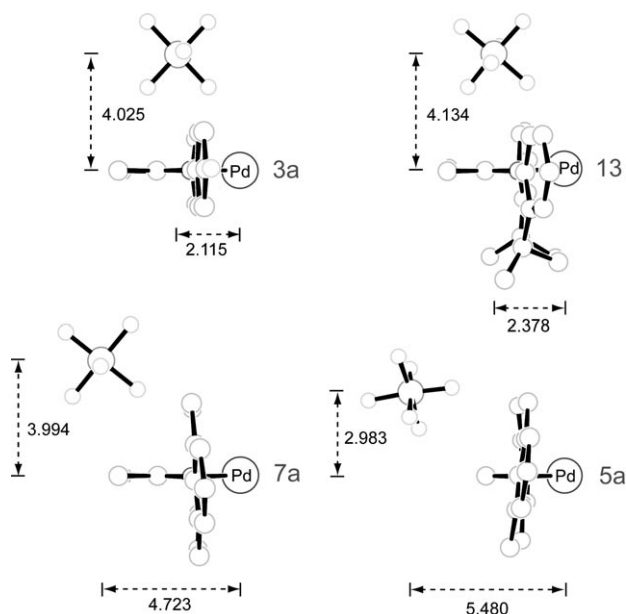

Figure 5. X-ray structures of complexes **3a**, **5a**, **7a**, and **13** showing the relative anion–cation position as a function of the structural features of the N,N ligands. Distances [Å] of the P atom of the anion from the [Pd–N(1)–C(22)–C(23)–N(2)] mean plane and the horizontal distance between the Pd atom and the intercept of the vertical distance are reported.

Table 1. CO/*p*-Methylstyrene copolymerization results.[a]

	Cat.	Yield [g][b]	CP [%]	gCP/gPd	Triads [%][c]			M_w ($\times 10^{-3}$) (M_w/M_n)
					ll	*ul/lu*	*uu*	
1	**1**	2.30	>99	154	31	49	20	17.7 (1.7)
2	**2**	2.90	>99	195	26	52	22	14.0 (1.7)
3	**3a**	3.20	>99	215	29	53	18	16.9 (1.6)
4[d]	**3a**	0.97	>99	65	31	53	16	14.7 (1.5)
5	**3b**	1.07	>99	72	32	52	16	12.4 (1.8)
6	**4**	1.36	82	75	36	51	13	17.2 (1.5)
7	**5a**	0.56	93	35	59	35	6	7.7 (1.5)
8	**5b**	0.60	>99	40	60	35	5	9.9 (1.6)
9	**6**	0.33	69	15	68	29	3	12.6 (1.4)
10	**7a**	0.45	59	18	75	24	1	8.0 (1.3)
11	**7b**	0.15	>99	10	80	20	<1	–
12[e]	**7b**	0.63	85	36	81	18	1	14.5 (1.6)
13[f]	**7b**	1.33	>99	89	80	19	1	20.2 (1.4)
14	**7c**	2.78	10	19	72	26	2	6.2 (1.2)
15	**8**	0.35	<1	<1	–	–	–	–
16	**9**	0.15	<1	<1	–	–	–	–
17	**11**	1.75	92	108	43	44	13	16.9 (1.1)
18	**12a**	1.87	87	109	47	43	10	16.1 (1.3)
19	**12b**	0.10	90	6	59	34	7	4.4 (1.3)
20	**12c**	2.64	98	174	30	57	13	12.6 (1.8)
21	**13**	0.59	45	18	50	43	7	9.6 (1.3)
22	**14**	1.65	<1	<1	–	–	–	–
23	**15**	0.90	>99	60	32	52	16	7.7 (1.6)

[a] Reaction conditions: $n_{Pd}=1.4\times10^{-4}$ mol; volume of *p*-methylstyrene: 5.5 mL (Pd:olefin=1:300); solvent: CH$_2$Cl$_2$ (5 mL); $T=17\,°C$; $P_{CO}=1$ atm; reaction time: 51 h. [b] In some cases a mixture of homo- and copolymer (CP) was obtained. [c] Evaluated from the intensities of the ^{13}C NMR *ipso*-carbon atom resonances. [d] $T=0\,°C$. [e] Reaction time = 150 h. [f] Reaction time = 150 h, $T=22\,°C$.

Productivities and molecular weights: The productivity of polyketone for the reported compounds decreases as the size of the aryl *ortho* substituents increases, going from 154 gCP/gPd (gCp/gPd = grams of copolymer per gram of palladium) for **1** (R^{2,6}=H, Table 1, entry 1) to zero with **8** and **9** (R^{2,6}=Et and *i*Pr, Table 1, entries 15 and 16, respectively). Only small amounts of homopolymer were obtained with the latter. An analogous decrease in catalytic activity was also observed with the *ortho*-monosubstituted compounds in the order **11** (R^2=Me)≈**12a** (R^2=Et)≫**13** (R^2=*i*Pr) (entries 17, 18, and 21, respectively).

The effect of ligand backbone modification on the catalyst performance was also studied using precatalysts **5a**, **6**, and **7a** (R^{2,6}=Me) and the productivity was found to follow the trend **5a** (R′=H) > **7a** (R′=Me) ≈ **6** (R′$_2$=An) (Table 1, entries 7, 10, and 9, respectively). The *para*-substituted complexes **3a** (R^4=F) and **2** (R^4=OMe) exhibit the highest catalytic activity, with productivities of 215 and 195 gCP/gPd, respectively. When the copolymerization was carried out using **4**, **14**, and **15** a fast formation of palladium metal was observed due to the low stability of the active species, and low polymeric yields were achieved.

The influence of the counterion on catalyst performance was investigated for compounds **3**, **5**, **7**, and **12**. In agreement with previous results,[13] the productivity of the copolymerization process is significantly affected by the coordinat-

ing ability of the anion[41] when the *para*-fluoro-substituted compound **3** is considered (Table 1, entries 3 and 5): the yield decreases from 215 to 72 gCP/gPd on passing from PF_6^- to the more coordinating $CF_3SO_3^-$, respectively. An analogous trend was observed with the productivities of **12a–c**, in which **12c**, which contains the very weakly coordinating BArF⁻ ion, is the most active catalyst. The anion effect on productivity is almost negligible when catalysts **5** (Table 1, entries 7 and 8) and **7** (Table 1, entries 10, 11,[42] and 14) are examined.

The molecular weights of the synthesized polyketones are only slightly influenced by the variation of the *N,N* ligand when systems without substituents in the *ortho* positions are considered, as demonstrated by the M_w values obtained with catalysts **1** ($R^4 = H$, $M_w = 17\,700$), **2** ($R^4 = OMe$, $M_w = 14\,000$), **3a** ($R^4 = F$, $M_w = 16\,900$), and **4** ($R^4 = CF_3$, $M_w = 17\,200$). However, the ligand effect is more pronounced when *ortho*-substituted compounds are used, and the molecular weights decrease as the axial sites of the catalysts become more hindered: **1** ($R^{2,6} = H$, $M_w = 17\,700$) ≈ **11** ($R^2 = Me$, $M_w = 16\,900$) ≈ **12a** ($R^2 = Et$, $M_w = 16\,100$) > **13** ($R^2 = iPr$, $M_w = 9600$) ≈ **7a** ($R^{2,6} = Me$, $M_w = 8000$). The molecular weight values also seem to be related to the coordinating ability of the anion, although in a different manner depending on the accessibility of the metal center. According to previous results with $[Pd(\eta^1,\eta^2-C_8H_{12}OMe)(2,2'-bipyridine)]X$,[13] in which the anion has the possibility of coming close to the palladium(II) metal, the most coordinating anion gives the lowest M_w [16\,900 with **3a** ($R^4 = F$, PF_6^-) and 12\,400 with **3b** ($R^4 = F$, $CF_3SO_3^-$); 16\,100 with **12a** ($R^2 = Et$, PF_6^-) and 4400 with **12b** ($R^2 = Et$, $CF_3SO_3^-$)]. Almost no effect was found for **5a** and **5b** [7700 with **5a** (PF_6^-) and 9900 with **5b** ($CF_3SO_3^-$)] where the counterion is confined to the back of the diimine ligand.

Copolymer stereochemistry: The polyketones were characterized by means of ¹H and ¹³C{¹H} NMR spectroscopy (1,1,1,3,3,3-hexafluoro-2-propanol/CDCl₃ 1/1 (v/v), 308 K). The tacticity of the copolymers was evaluated by integrating the ¹³C{¹H} NMR resonances corresponding to the *ipso* carbon atoms of the tolyl groups.

Catalysts **1–4** afford regioregular polyketones with a "quasi-atactic" microstructure,[14,43–45] (Table 1, entries 1–6), whereas a remarkable increment of the isotactic *ll* component is observed with complexes **5–7**, which bear Me groups in the *ortho* positions (80% for complex **7b**). A slight prevalence for the *ll* triad (that increases with the size of R^2) is also observed for the copolymers produced by the *ortho*-monosubstituted compounds **11–13**. Changes in the α-diimine backbone affect the polymer microstructure according to the order $Me_2 > An > H_2$ (Table 1, entries 7, 9, and 10 or 8 and 11). The counterion significantly affects the stereoregularity of the copolymers: the isotactic content follows the coordinating ability of the anion, as evidenced by data collected for catalysts **7** and **12** (Table 1). While the use of BArF⁻ (**7c**) and PF_6^- (**7a**) results in similar amounts of the *ll* triad (72% and 75%, respectively), catalyst **7b**, which contains

the more coordinating $CF_3SO_3^-$ anion, affords a polyketone in which the *ll* content is as high as 80%. The ion-pairing effect is even more marked when the *ortho*-monosubstituted catalyst **12** is considered, with a notable increase of the isotactic component on going from BArF⁻ (**12c**, 30% *ll* triad) to $CF_3SO_3^-$ (**12b**, 59% *ll* triad; Figure 6). The influence of the anion on the microstructure is negligible when the catalysts **3a** and **3b**, or **5a** and **5b** are compared.
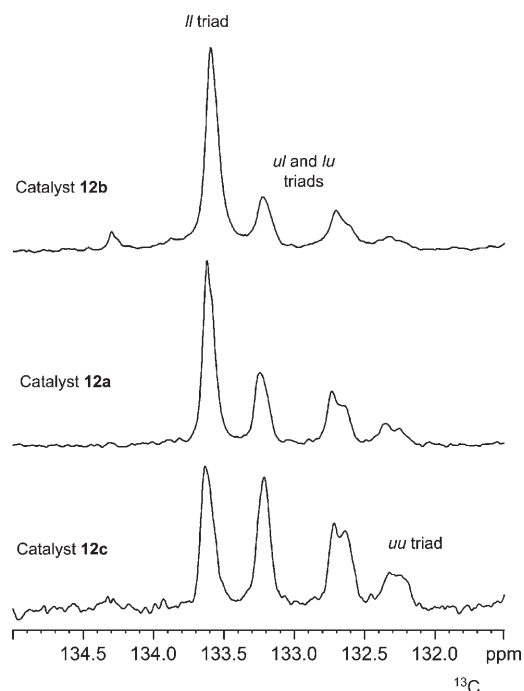

Figure 6. Section of the ¹³C{¹H} NMR spectrum (100.61 MHz, 308 K, $(CF_3)_2CHOH/CDCl_3$ 1/1 (v/v)) relative to the *ipso*-carbon resonances of CO/*p*-methylstyrene polyketones produced by complexes **12a** ($X^- = PF_6^-$), **12b** ($X^- = CF_3SO_3^-$) and **12c** ($X^- = BArF^-$).

Discussion

Complexes **1–15** have been shown to be particularly suitable for investigating the counterion/ligand interplay in the copolymerization of CO and *p*-methylstyrene since both their interionic structure and catalytic performance are sensitive to small variations in the steric and electronic properties of the diimine ligands and counterion.

Activity: The results reported here regarding the activity of catalysts **1–15** towards the copolymerization of CO and *p*-methylstyrene clearly indicate that more electron-donating diimine ligands with a reduced encumbrance in the apical positions[27,45,46] afford the highest yield and molecular weights.

It is well-known that aryl-substituted α-diimine ligands in square-planar complexes orient the aryl rings almost perpendicularly to the coordination plane and direct the *ortho* substituents in the apical positions.[24,29,30,47–49] Consequently, the size of the *ortho* substituents plays the greatest role in

the steric hindrance in the apical positions although the counterion and the R′ substituent on the back also play a role. The latter acts indirectly by altering the perpendicularity of the aryl moiety with respect to the coordination plane. Thus, when R′ is small (as in **5a**) the aryl has the possibility of inclining and relieving part of the steric hindrance in the apical positions. This is reflected in a beneficial effect on the catalytic activity. The productivity trend observed for the *ortho*-dimethyl-substituted ligands is in perfect agreement with this consideration: **5a** > **6** ≈ **7a**.

The role of the counterion on the activity of palladium(II) catalysts bearing flat N,N ligands has been investigated in depth previously.[13] It was found that the more coordinating the counterion, the less active the catalyst. This is not always true in catalysts **1**–**15** because it depends on the location of the anion with respect to the cationic moiety and, particularly, whether or not the anion is near the metal center. This is dictated by the N,N ligand. Interionic ^{19}F,^{1}H-HOESY NMR and X-ray studies have shown that the anion can approach the metal center for catalysts having H in the *ortho* positions. For these catalysts the anion drastically affects the activity in the usual way: an increase of the coordinating ability of the anion reduces the catalytic activity. On the other hand, no counterion effect was observed when catalysts with methyl groups in the *ortho* positions were considered. In these catalysts, solution ^{19}F,^{1}H-HOESY NMR and X-ray studies in the solid state showed that the anion is confined above the N=C−C=N moiety, at the back of the aryl "wall" and therefore far away from the metal center. To the best of our knowledge this is the first example to show that the variation of the counterion position is directly related to a change in the catalytic activity.

The rationalization of the steric effect on the activity of hemi-hindered catalysts **11**–**15** is rather complicated due to the presence of the four isomers shown in Scheme 2. In-depth NMR studies at low temperature allowed the two most abundant isomers, which have the *ortho* R substituents oriented in the same direction (*c* and *d* in Scheme 2), to be identified. Rather counter-intuitively, the percentage of *c* increases significantly as the encumbrance of the *ortho* R group increases [52% with R^2=Me (**11**), 58% with R^2=Et (**12a**), and 64% with R^2=*i*Pr (**13**)]. An increase in the amount of *c* isomer is also observed when a more coordinating counterion is used. The greater stability of isomers *c* and *d* with respect to *a* and *b* is due to the different anion–cation interactions: the higher the steric hindrance in the apical position, the higher the difference in the energy of the anion/cation interactions in the C_2 and C_s isomers. The decreased activity observed with an increase of the steric hindrance in the apical position can be explained by assuming that the C_s-symmetric ligand has a smaller productivity than the C_2-symmetric one,[50] as observed in both CO/styrene copolymerization[14] and polymerization of propylene.[51] It is also reasonable that an increase of the coordinating ability of the counterion reduces the activity of C_s-symmetric catalysts more than C_2-symmetric ones, therefore in *ortho*-monosubstituted catalysts the counterion exerts a

twofold role by decreasing the rate of copolymerization of the individual isomers in a differential way and changing the relative amounts of the four possible isomers.

The electronic properties[52,53] of diimine ligands are also important for the productivity of the catalysts. This can be clearly seen in the results of catalysts **1**–**4**, which can be reasonably considered isosteric as far as the hindrance in the apical positions is concerned. The following trend of productivity was observed: **3a** (R^4=F) > **2** (R^4=OMe) > **1** (R^4= H) ≫ **4** (R^4=CF$_3$). Therefore, more electron-donating diimine ligands increase the catalytic activity. This means that the thermodynamic stabilization is the critical factor for these catalysts. The analogous compounds $[Pd(\eta^1,\eta^2-C_8H_{12}OMe)(2,2′-bipyridine)]X$,[13] which bear the more basic bipy ligand, consistently afford a productivity that is higher than that observed with compounds **3a** and **2**, while compounds with less electron-donating N,N [54] or N,O ligands[55] are only marginally or not active at all.

Stereoregularity: The *ortho*-disubstituted catalysts **1**–**10** are rather peculiar since they allow atactic or isotactic CO/*p*-methylstyrene copolymers to be produced using achiral ligands, that is, through a chain-end control of the stereochemistry. This is in sharp contrast to all the other achiral catalysts for stereospecific CO/styrene copolymerization, which lead to syndiotactic copolymers. The degree of isotacticity increases with an increase of the rigidity of the aryl moieties of the diimines. This can occur by using more sterically demanding R^2 or R′ groups or more coordinating counterions. All three of these factors are beneficial for the stereoregularity of the copolymer but are, at the same time, detrimental for the activity of the catalysts. This is clearly shown by **7b**, which gives the highest degree of isotacticity (*ll*=81%) but with only a modest productivity (9 gCP/gPd). The interplay between R′ substituents and the counterion is notable. When R′=Me (**7**) a small but clear effect of the counterion is present, with the amount of *ll* triads going from 75% for PF$_6^-$ (**7a**) to 81% for CF$_3$SO$_3^-$(**7b**). On the contrary the counterion does not affect the isotacticity when R′=H (**5**) [*ll*=59% for PF$_6^-$ (**5a**); *ll*=60% for CF$_3$SO$_3^-$ (**5b**)]. This subtle counterion/ligand interplay can be nicely rationalized by considering the interionic structure of catalysts **5a** and **7a**. As shown in Figure 5, the anion in catalysts **5a** is farther away from the aryl rings than in **7a** and cannot exert its pivotal role in making the aryls more rigid.

Although catalysts with *ortho*-monosubstituted diimines produce less stereoregular copolymers they exhibit very interesting aspects concerning the ligand/counterion interplay. As stated above, in *ortho*-monosubstituted catalysts the counterion exerts a kinetic role that decreases, in a differential way, the rate of copolymerization of the individual isomers, and a thermodynamic role that changes the relative amounts of the four possible isomers. Both of these can clearly affect the stereoregularity of the copolymer since the diimine ligand in isomers *a* and *b* has C_2 symmetry. It seems reasonable to hypothesize that they produce more isotactic copolymers than isomers *c* and *d* (C_s symmetry) through an

enantiomorphic site-control mechanism. An increase in the size of the *ortho* substituents, i.e. passing from **11** to **13**, only causes a marginal increase in the isotacticity of the copolymer, probably because the more isotactic copolymer produced by C_2-symmetric complexes prevails over the higher percentage of C_s-symmetric catalyst. A variation of the counterion in catalyst **12** has a considerable effect on the isotacticity, which varies from 30% (BArF$^-$) to 59% (CF$_3$SO$_3^-$) *ll* content. At the same time, the percentage of C_2-symmetric catalysts decreases as the coordinating ability of the counterion increases. This clearly means that the kinetic role of the counterion overcomes the thermodynamic one. Consequently, as shown in Scheme 3, as the counterion

THERMODYNAMICS vs. KINETICS
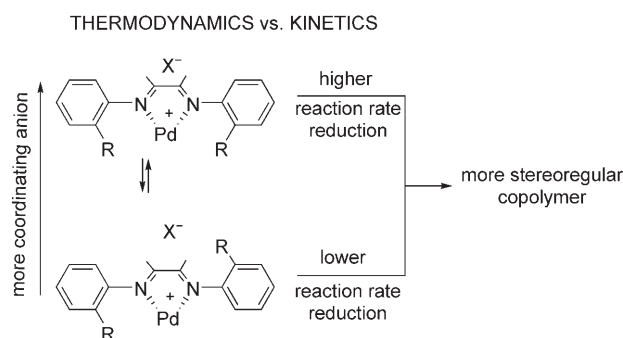
Scheme 3.

becomes more coordinating the amount of C_s-symmetric isomers, which produce a less stereoregular copolymer, increases. Their reaction rates, however, reduce much more than those of the least abundant C_2-symmetric isomers and, in the end, the copolymer is more stereoregular.

Conclusion

Herein we have shown the importance of the structural interionic information derived from ^{19}F,^{1}H-HOESY NMR spectroscopy and X-ray single crystal diffractometry for understanding the interplay between the counterion and the ligand in the copolymerization of CO and *p*-methylstyrene catalyzed by the Pd complexes **1–16**.

A remarkable agreement has been observed between the interionic structural modifications dictated by changing the ligand or the anion and the changes in the catalytic performances. This has led to an unprecedented detection of a different dependence of the catalyst productivity on changing the anion position. In fact, in catalysts **1–4**, where the counterion is located in the apical positions, its nature strongly affects the productivity. On the contrary, in complexes **5–7** the access of the counterion to the apical positions is inhibited by the *ortho*-methyl substituents, which means that it has little effect on the productivity. The counterion/ligand interplay in the stereoselectivity of catalysts **1–10** is even more subtle but is perfectly understandable based on the interionic structure. The highest degree of isotacticity was obtained

with catalyst **7b**, which has methyl groups in both the *ortho* positions and in the back, and CF$_3$SO$_3^-$, which is the most coordinating counterion. Remarkably, the stereoselectivity of catalyst **5**, which differs from **7** in that R′ is hydrogen instead of methyl, is independent of the counterion since it is 0.75 Å further away than in **7a** and cannot contribute to making the aryl ring more rigid.

Finally, the counterion effect on the isotacticity has been found to be considerable in the *ortho*-monosubstituted catalysts **11–16**; for example, the *ll* content of 30% for **12c** (X$^-$ = BArF$^-$) increases to 59% for **12b** (CF$_3$SO$_3^-$). Interionic structural studies have indicated that the C_s-symmetric isomers are thermodynamically favored as the coordinating ability of the counterion increases. Since C_2-symmetric isomers should afford more isotactic copolymers than C_s-symmetric ones, it can be deduced that the decrease of the copolymerization rate for the former on increasing the coordinating ability of the counterion is much lower than that of the latter. Therefore, the counterion kinetic effect prevails over the thermodynamic one.

Experimental Section

General: Manipulation of all complexes was carried out by employing standard Schlenk techniques and a dry, oxygen-free nitrogen atmosphere. Solvents were dried and purified by standard methods and freshly distilled under nitrogen. The NMR solvents were deoxygenated by repeated freeze–pump–thaw cycles, and stored over molecular sieves (4 Å). *p*-Methylstyrene was dried over calcium hydride and distilled before use. The other CP-grade chemicals were used as received. Carbon monoxide (CP grade 99.99%) was supplied by Air Liquide. The ligands Ar−N=C(R′)−C(R′)=N−Ar (R′=H, Me;[56] R′$_2$=9-anthryl[57]), (4S,4S')-(−)-4,4′,5,5′-tetrahydro-4,4′-bis(1-methylethyl)-2,2′-bisoxazole,[58–60] and *i*PrN=C(H)−C(H)=N*i*Pr,[61] complexes [PdCl$_2$(C$_8$H$_{12}$)], [Pd(η^1,η^2-C$_8$H$_{12}$OMe)Cl]$_2$,[62,63] and **1**, **7a**, **8**, and **9**,[23] and [{3,5-(CF$_3$)$_2$-C$_6$H$_3$}$_4$B]$^-$Na$^+$[64] were synthesized according to literature procedures. Compounds **2–6**, **7b**, and **7c** were prepared as previously communicated.[20] Elemental analyses (C, H, N) were carried out with a Fisons Instruments 1108 CHNS-O elemental analyzer. IR spectra were measured at room temperature in CHCl$_3$ solution, on a FTIR 1725 X Perkin-Elmer spectrophotometer. One- and two-dimensional ^{1}H, ^{13}C, and ^{19}F NMR spectra were measured with a Bruker DRX 400 spectrometer. The spectra were referenced relative to TMS (^{1}H and ^{13}C) or CFCl$_3$ (^{19}F). NMR samples were prepared by dissolving about 20 mg of the compound in 0.5 mL of CD$_2$Cl$_2$. Two-dimensional ^{1}H-NOESY and ^{19}F,^{1}H-HOESY spectra were recorded with a mixing time of 500–800 ms. For the CO/*p*-methylstyrene copolymer characterization, NMR samples were prepared by dissolving about 35 mg of the copolymer in a mixture of (CF$_3$)$_2$CHOH (HFIP) and CDCl$_3$ (1/1, v/v). **CAUTION: HFIP is a very volatile and highly toxic solvent, so proper protection should be used when it is handled.** The molecular weights (M_w) of polymers and the molecular weight distributions (M_w/M_n) were determined by gel permeation chromatography versus polystyrene standards. The analyses were recorded with a Knauer HPLC (K-501 Pump, K-2501 UV-detector) with a PLgel 5 µm 10^4 Å GPC column and chloroform as solvent (flow rate: 0.6 mL min^{-1}). Samples were prepared by dissolving 2 mg of the copolymer in CHCl$_3$ (10 mL). The statistical calculations were performed using the Bruker Chromstar software program.

NMR characterization of α-diimine ligands

***N*,*N'*-(1,2-Dimethyl-1,2-ethanediylidene)bis(2,4,6-trifluoro)benzenamine**: ^{1}H NMR (400 MHz, CD$_2$Cl$_2$, 25°C): δ = 2.23 (t, $^6J_{H,F}$ = 1.24 Hz, 6H; H19), 6.85 ppm (m, 4H; H11 and H11a); ^{19}F NMR (376 MHz, CD$_2$Cl$_2$, 25°C):

$\delta = -120.7$ (br. m, 4F; F10 and F10a), -115.4 ppm (m, 2F; F12); elemental analysis calcd (%) for $C_{16}H_{10}F_6N_2$ (344.3): C 55.82, H 2.93, N 8.14; found: C 56.40, H 2.97, N 8.38.

N,N′-(1,2-Dimethyl-1,2-ethanediylidene)bis(2,4-difluoro)benzenamine:
^{1}H NMR (400 MHz, CD_2Cl_2, 25°C): $\delta = 2.18$ (d, $^6J_{H,F} = 1.47$ Hz, 6H; H19), 6.90 (m, 2H; H10a), 6.98 ppm (m, 4H; H11 and H11a); ^{19}F NMR (376 MHz, CD_2Cl_2, 25°C): $\delta = -117.5$ (br. m, 2F; F10 or F12), -122.5 ppm (br. m, 2F; F12 or F10); elemental analysis calcd (%) for $C_{16}H_{12}F_4N_2$ (308.3): C 62.34, H 3.92, N 9.09; found: C 62.84, H 3.94, N 9.36.

N,N′-(1,2-Dimethyl-1,2-ethanediylidene)bis(2-trifluoromethyl)benzenamine: ^{1}H NMR (400 MHz, CD_2Cl_2, 25°C): $\delta = 2.15$ (s, 6H; H19), 6.83 (d, $^3J_{H,H} = 7.85$ Hz, 2H; H11 or H10a), 7.73 (d, $^3J_{H,H} = 7.83$ Hz, 2H; H10a or H11), 7.27 (t, $^3J_{H,H} = 7.65$ Hz, 2H; H12 or H11a), 7.60 ppm (t, $^3J_{H,H} = 7.60$ Hz, 2H; H11a or H12); ^{13}C NMR (100 MHz, CD_2Cl_2, 25°C): $\delta = 169.51$ (s; C17), 149.33 (s; C9), 133.17 (s; C12), 126.76 (q, $^3J_{C,F} = 5.13$ Hz; C11), 124.35 (q, $^1J_{C,F} = 172.9$ Hz; C21), 124.01 (s; C10a), 119.39 (s; C11a), 119.35 (9, $^2J_{C,F} = 30.19$ Hz; C10), 16.01 ppm (s; C19); ^{19}F NMR (376 MHz, CD_2Cl_2, 25°C): $\delta = -62.72$ ppm (s, 6F; F21); elemental analysis calcd (%) for $C_{18}H_{14}F_6N_2$ (372.3): C 58.07, H 3.79, N 7.52; found: C 58.67, H 3.98, N 7.53.

N,N′-(1,2-Dimethyl-1,2-ethanediylidene)bis(3,4-difluoro)benzenamine:
^{1}H NMR (400 MHz, CD_2Cl_2, 25°C): $\delta = 2.15$ (s, 6H; H19), 6.55, 6.69, 7.23 ppm (m, 6H; H10, H10a and H11a); ^{19}F NMR (376 MHz, CD_2Cl_2, 25°C): $\delta = -138.1$ (m, 2F; F11 or F12), -146.1 ppm (m, 2F; F12 or F11); elemental analysis calcd (%) for $C_{16}H_{12}F_4N_2$ (308.3): C 62.34, H 3.92, N 9.09; found: C 62.65, H 3.98, N 9.60.

Preparation and characterization of palladium(II) complexes

Complex 2: Complex **2** was synthesized according to a literature procedure[23] from $[Pd(\eta^1,\eta^2-C_8H_{12}OMe)Cl]_2$ (100 mg, 0.18 mmol), N,N′-(1,2-dimethyl-1,2-ethanediylidene)bis(4-methoxy)benzenamine (105 mg, 0.36 mmol), and NH_4PF_6 (150 mg). It was isolated as a yellow powder (200 mg, 0.29 mmol; yield 81%). ^{1}H NMR (400 MHz, CD_2Cl_2, 29°C): $\delta = 7.07$ (m, 8H; H10a, H11a, H11, H10, H14a, H15a, H15 and H14), 5.53 (m, 1H; H1), 5.06 (m, 1H; H2), 3.87 (s, 6H; Ph-OCH_3), 3.22 (m, 1H; H5), 2.66 (s, 3H; OMe), 2.57 (m, 2H; H3 and H3′), 2.31 (m, 7H; H6, H19 and H20), 2.17 (m, 3H; H7, H8 and H8′), 1.88 (m, 2H; H4 and H4′), 1.48 ppm (m, 1H; H7′); ^{13}C{^{1}H} NMR (100 MHz, CD_2Cl_2, 29°C): $\delta = 158.9$ (s; C12 and C16), 138.8 (br, C9 and C13), 121.7 (s; C10a, C10, C14a and C14), 115.2 (s; C11a, C11, C15a and C15), 109.7 (s; C1), 108.6 (s; C2), 81.1 (s; C5), 55.8 (s, Ph-OCH_3), 55.6 (s, OMe), 55.1 (s; C6), 32.9 (s; C7), 31.4 (s; C4), 28.5 (s; C3), 26.2 (s; C8), 20.3 ppm (br, C19 and C20); elemental analysis calcd (%) for $C_{27}H_{35}F_6N_2O_3PPd$ (687): C 47.21, H 5.14, N 4.08; found: C 48.00, H 5.20, N 4.11.

Complex 3a: Complex **3a** was synthesized according to a literature procedure[23] from $[Pd(\eta^1,\eta^2-C_8H_{12}OMe)Cl]_2$ (100 mg, 0.18 mmol), N,N′-(1,2-dimethyl-1,2-ethanediylidene)bis(4-fluoro)benzenamine (98 mg, 0.36 mmol), and NH_4PF_6 (150 mg). It was isolated as a yellow powder (198 mg, 0.30 mmol; yield 84%). ^{1}H NMR (400 MHz, CD_2Cl_2, 29°C): $\delta = 7.24–7.29$ (t, $^3J_{H,H} = 8.8$ Hz, 4H; H11a, H11, H15a, and H15), 7.14 (br, 4H; H10a, H10, H14a, and H14), 5.46 (m, 1H; H1), 5.02 (m, 1H; H2), 3.19 (m, 1H; H5), 2.66 (s, 3H; OMe), 2.63 (m, 1H; H3′), 2.55 (m, 1H; H3), 2.28 (br m, 7H; H6, H19, and H20), 2.15 (m, 3H; H7, H8, and H8′), 1.88 (m, 2H; H4 and H4′), 1.63 ppm (m, 1H; H7′); ^{13}C{^{1}H} NMR (100 MHz, CD_2Cl_2, 29°C): $\delta = 175.5–180.0$ (br, C17 and C18), 161.6 (d, $^1J_{C,F} = 246$ Hz; C12 and C16), 142.1 (br, C9 and C13), 122.5 (br, C10a, C10, C14a, and C14), 117.3 (d, $^1J_{C,F} = 23.1$ Hz; C11a, C11, C15a and C15), 109.9 (s; C1), 108.8 (s; C2), 81.1 (s; C5), 55.7 (s, OMe), 55.4 (s; C6), 33.2 (s; C7), 31.5 (s; C4), 28.6 (s; C3), 26.3 (s; C8), 20.6 ppm (br, C19 and C20); ^{19}F NMR (376 MHz, CD_2Cl_2, 29°C): $\delta = -115.45$ (br, 2F; p-F), -72.5 ppm (d, $^1J_{F,P} = 713$ Hz, 6F; PF_6^-); ^{31}P NMR (162 MHz, CD_2Cl_2, 29°C): $\delta = -72.50$ ppm (d, $^1J_{F,P} = 711.8$ Hz, 1P; PF_6^-); elemental analysis calcd (%) for $C_{25}H_{29}F_8N_2OPPd$ (662.9): C 45.30, H 4.41, N 4.23; found C 45.90, H 4.53, N 4.25.

Complex 3b: N,N′-(1,2-Dimethyl-1,2-ethanediylidene)bis(4-fluoro)benzenamine (100 mg, 0.37 mmol) was added to a stirred solution of $[Pd(\eta^1,\eta^2-C_8H_{12}OMe)Cl]_2$ (100 mg, 0.18 mmol) in dichloromethane (5 mL) at 25°C. After 5 min the obtained solution was transferred into a

Schlenk tube containing $AgCF_3SO_3$ (98 mg, 0.38 mmol) and allowed to react for 1 h, during which time AgCl precipitated. The mixture was filtered through Celite and a yellow solid was obtained after evaporation of the solvent under vacuum. This solid gave compound **3b** as a yellow powder (213 mg, 0.32 mmol; yield 90%) upon treatment with hexane (3× 5 mL). ^{1}H NMR (400 MHz, CD_2Cl_2, 0°C): $\delta = 7.27–7.09$ (br, 8H; H10, H10a, H11, H11a, H14, H14a, H15, and H15a), 5.40 (m, 1H; H1), 4.97 (m, 1H; H2), 3.18 (m, 1H; H5), 2.65 (m, 1H; H3′), 2.61 (s, 3H; OMe), 2.48 (m, 1H; H3), 2.28 (br m, 7H; H6, H19, and H20), 2.14 (m, 3H; H7, H8 and H8′), 1.86 (m, 2H; H4 and H4′), 1.41 ppm (m, 1H; H7′); ^{19}F NMR (376 MHz, CD_2Cl_2, 0°C): $\delta = -115.85$ (br, 2F; p-F), -79.2 ppm (s, 3F; $CF_3SO_3^-$); elemental analysis calcd (%) for $C_{26}H_{29}F_5N_2O_4PdS$ (667): C 46.82, H 4.38, N 4.20; found: C 47.10, H 4.41, N 4.20.

Complex 4: Complex **4** was synthesized according to a literature procedure[23] from $[Pd(\eta^1,\eta^2-C_8H_{12}OMe)Cl]_2$ (100 mg, 0.18 mmol), N,N′-(1,2-dimethyl-1,2-ethanediylidene)bis(4-trifluoromethyl)benzenamine (150 mg, 0.40 mmol), and NH_4PF_6 (150 mg). It was isolated as a yellow powder (184 mg, 0.24 mmol; yield 67%). ^{1}H NMR (400 MHz, CD_2Cl_2, 29°C): $\delta = 7.86$ (d, $^3J_{H,H} = 8.46$ Hz, 4H; H11a, H11, H15a, and H15), 7.32 (br d, 4H; H10a, H10, H14a, and H14), 5.44 (m, 1H; H1), 5.04 (m, 1H; H2), 3.13 (m, 1H; H5), 2.63 (m, 1H; H3), 2.55 (s, 3H; OMe), 2.52 (m, 1H; H3′), 2.31 (s, 6H; H19 and H20), 2.24 (m, 1H; H6), 2.17 (m, 3H; H7, H8 and H8′), 1.88 (m, 2H; H4 and H4′), 1.43 ppm (m, 1H; H7′); ^{13}C{^{1}H} NMR (100 MHz, CD_2Cl_2, 29°C): $\delta = 183.1$ (s; C17 or C18), 179.0 (s; C18 or C17), 148.8 (s; C9 and C13), 129.9 (d, $^2J_{C,F} = 32.9$ Hz; C12 and C16), 124.1 (q, $^1J_{C,F} = 272.1$ Hz; CF_3), 127.8 (s; C10a, C10, C14a, and C14), 121.4 (m, C11a, C11, C15a, and C15), 110.0 (s; C1), 109.2 (s; C2), 80.9 (s; C5), 56.0 (OMe), 55.6 (s; C6), 33.3 (s; C7), 31.5 (s; C4), 28.6 (s; C3), 26.1 (s; C8), 20.8 ppm (C19 and C20); ^{19}F NMR (376 MHz, CD_2Cl_2, 29°C): $\delta = -72.20$ (d, $^1J_{F,P} = 712.91$ Hz, 6F; PF_6^-), -63.41 ppm (s; CF_3); elemental analysis calcd (%) for $C_{27}H_{29}F_{12}N_2OPPd$ (372.3): C 42.51, H 3.83, N 3.67; found: C 42.58, H 3.91, N 3.68.

Complex 5a: Complex **5a** was synthesized according to a literature procedure[23] from $[Pd(\eta^1,\eta^2-C_8H_{12}OMe)Cl]_2$ (100 mg, 0.18 mmol), N,N′-(1,2-ethanediylidene)bis(2,6-dimethyl)benzenamine (98 mg, 0.37 mmol), and NH_4PF_6 (150 mg). It was isolated as a yellow powder (210 mg, 0.32 mmol; yield 90%). ^{1}H NMR (400 MHz, CD_2Cl_2, −40°C): $\delta = 8.48$ (s, 1H; H18), 8.32 (s, 1H; H17), 7.26–7.15 (br, 6H; H11, H11a, H12, H15, H15a, and H16), 5.59 (m, 1H; H1), 4.90 (m, 1H; H2), 3.08 (m, 1H; H5), 2.65 (m, 1H; H3), 2.47 (m, 1H; H3′), 2.38 (s, 3H; OMe), 2.33 (s, 3H; H21), 2.31 (s, 3H; H23), 2.30 (s, 3H; H22), 2.19 (s, 3H; H24), 2.13 (br m, 4H; H7, H8, H8′, and H6), 1.86 (m, 2H; H4 and H4′), 1.45 ppm (m, 1H; H7′); ^{13}C{^{1}H} NMR (100 MHz, CD_2Cl_2, −40°C): $\delta = 171.4$ (s; C17), 166.5 (s; C18), 144.5 (s; C9), 144.1 (s; C13), 130.0, 129.6, 129.3, 129.2, 129.1, 128.7, 128.5, 128.1, 127.8, 127.6 (C10, C10a, C11, C11a, C12, C14, C14a, C15, C15a, C16), 113.4 (s; C1), 110.6 (s; C2), 82.1 (s; C5), 57.4 (s; C6), 55.9 (s, OMe), 34.3 (s; C7), 31.5 (s; C4), 29.8 (s; C3), 26.6 (s; C8), 18.9 (s; C21), 18.6 (s; C22 and C23), 18.2 ppm (s; C24). ^{19}F NMR (376 MHz, CD_2Cl_2, −40°C): $\delta = -72.8$ ppm (d, $^1J_{F,P} = 712$ Hz, 6F; PF_6^-); elemental analysis calcd (%) for $C_{27}H_{35}F_6N_2OPPd$ (655): C 49.51, H 5.39, N 4.28; found: C 49.58, H 5.41, N 4.30.

Complex 5b: Complex **5b** was synthesized according to the procedure described for **3b** using $[Pd(\eta^1,\eta^2-C_8H_{12}OMe)Cl]_2$ (100 mg, 0.18 mmol), N,N′-(1,2-ethanediylidene)bis(2,6-dimethyl)benzenamine (98 mg, 0.37 mmol), and $AgCF_3SO_3$ (98 mg, 0.38 mmol). It was isolated as a yellow powder (204 mg, 0.31 mmol; yield 86%). ^{1}H NMR (400 MHz, CD_2Cl_2, −40°C): $\delta = 8.60$ (s, 1H; H18), 8.43 (s, 1H; H17), 7.24–7.18 (br, 6H; H11, H11a, H12, H15, H15a, and H16), 5.56 (m, 1H; H1), 4.88 (m, 1H; H2), 3.08 (m, 1H; H5), 2.66 (m, 1H; H3), 2.48 (m, 1H; H3′), 2.39 (s, 3H; OMe), 2.35 (s, 3H; H21), 2.31 (s, 6H; H22 and H23), 2.21 (s, 3H; H24), 2.15 (br m, 4H; H7, H8, H8′, and H6), 1.86 (m, 2H; H4 and H4′), 1.45 ppm (m, 1H; H7′); ^{13}C{^{1}H} NMR (100 MHz, CD_2Cl_2, −40°C): $\delta = 172.1$ (s; C17), 167.2 (s; C18), 144.6 (s; C9), 144.2 (s; C13), 130.0, 129.5, 129.2, 129.1, 129.0, 128.6, 128.5, 128.0, 127.8 (C10, C10a, C11, C11a, C12, C14, C14a, C15, C15a, C16), 120.9 (q, $^1J_{C,F} = 320.6$ Hz; CF_3SO_3), 113.1 (s; C1), 110.3 (s; C2), 82.1 (s; C5), 57.1 (s; C6), 55.8 (s, OMe), 34.3 (s; C7), 31.5 (s; C4), 29.8 (s; C3), 26.6 (s; C8), 18.9 (s; C21), 18.7 (s; C22), 18.6 (s; C23), 18.3 ppm (s; C24); ^{19}F NMR (376 MHz, CD_2Cl_2, −40°C): $\delta =$

−79.7 ppm (s, 3F; CF$_3$SO$_3$$^-$); elemental analysis calcd (%) for C$_{28}$H$_{35}$F$_3$N$_2$O$_4$PdS (659.1): C 51.03, H 5.35, N 4.25; found: C 52.00, H 5.46, N 4.25.

Complex 6: Complex **6** was synthesized according to a literature procedure[23] from [Pd(η^1,η^2-C$_8$H$_{12}$OMe)Cl]$_2$ (100 mg, 0.18 mmol), N,N'-(1,2-acenaphthylenediylidene)bis(2,6-dimethyl)benzenamine (144 mg, 0.37 mmol), and NH$_4$PF$_6$ (150 mg). It was isolated as an orange powder (249 mg, 0.32 mmol; yield 90%). ^{1}H NMR (400 MHz, CD$_2$Cl$_2$, −40°C): δ = 8.27 (d, $^3J_{H,H}$ = 8.3 Hz, 1H; H31), 8.21 (d, $^3J_{H,H}$ = 8.3 Hz, 1H; H33), 7.59 (m, 2H; H30 and H34), 7.47–7.30 (br, 6H; H11, H11a, H12, H15, H15a, and H16), 6.75 (d, $^3J_{H,H}$ = 7.3 Hz, 1H; H35), 6.71 (d, $^3J_{H,H}$ = 8.3 Hz, 1H; H29), 5.72 (m, 1H; H1), 5.00 (m, 1H; H2), 3.23 (m, 1H; H5), 2.73 (m, 1H; H3), 2.64 (m, 1H; H3'), 2.47 (s, 3H; OMe), 2.39 (s, 3H; H21), 2.36 (s, 3H; H23), 2.31 (s, 3H; H22), 2.28 (brm, 4H; H7, H8, H8' and H6), 2.26 (3H; H24), 1.90 (m, 2H; H4 and H4'), 1.50 ppm (m, 1H; H7'); ^{13}C{^{1}H} NMR (100 MHz, CD$_2$Cl$_2$, −40°C): δ = 175.3 (s; C17), 170.4 (s; C18), 146.7 (s; C36), 142.3 (s; C9), 142.0 (s; C13), 134.4 (s; C31), 133.4 (s; C33), 131.5, 130.5, 130.14, 130.12, 130.08, 130.07, 129.9, 129.4, 129.0, 128.3, 128.2, 127.33, 127.29, 125.16, 125.12 (C10, C10a, C11, C11a, C12, C14, C14a, C15, C15a, C16, C19, C20, C30, C32, C34), 126.5 (s; C29), 125.7 (s; C35), 112.4 (s; C1), 109.7 (s; C2), 82.2 (s; C5), 58.2 (s; C6), 55.9 (s, OMe), 34.4 (s; C7), 31.6 (s; C4), 29.9 (s; C3), 26.8 (s; C8), 18.8 (s; C21), 18.52 (s; C23), 18.48 (s; C22), 18.2 ppm (s; C24); ^{19}F NMR (376 MHz, CD$_2$Cl$_2$, −40°C): δ = −73.7 ppm (d, $^1J_{F,P}$ = 712 Hz, 6F; PF$_6$$^-$); elemental analysis calcd (%) for C$_{37}$H$_{39}$F$_6$N$_2$OPPd (779.1): C 57.04, H 5.05, N 3.60; found: C 57.08, H 5.11, N 3.68.

Complex 7b: Complex **7b** was synthesized according to the procedure described for **3b** using [Pd(η^1,η^2-C$_8$H$_{12}$OMe)Cl]$_2$ (100 mg, 0.36 mmol), N,N'-(1,2-dimethyl-1,2-ethanediylidene)bis(2,6-dimethyl)benzenamine (108 mg, 0.37 mmol), and AgCF$_3$SO$_3$ (98 mg, 0.38 mmol). It was isolated as a yellow powder (234 mg, 0.34 mmol; yield 95%). ^{1}H NMR (400 MHz, CD$_2$Cl$_2$, −10°C): δ = 7.28–7.14 (br, 6H; H11, H11a, H12, H15, H15a, and H16), 5.31 (m, 1H; H1), 4.69 (m, 1H; H2), 3.01 (m, 1H; H5), 2.62 (m, 1H; H3), 2.48 (m, 1H; H3'), 2.42 (s, 3H; OMe), 2.36 (s, 3H; H19 or H20), 2.31 (s, 3H; H21), 2.30 (s, 3H; H23), 2.27 (s, 3H; H22), 2.25 (s, 3H; H20 or H19), 2.15 (s, 3H; H24), 2.09 (brm, 3H; H7, H8, and H8'), 1.91 (m, 1H; H6), 1.84 (m, 2H; H4 and H4'), 1.42 ppm (m, 1H; H7'); ^{19}F NMR (376 MHz, CD$_2$Cl$_2$, −10°C): δ = −79.4 ppm (s, 3F; CF$_3$SO$_3$$^-$); elemental analysis calcd (%) for C$_{30}$H$_{39}$F$_3$N$_2$O$_4$PdS (687.1): C 52.44, H 5.72, N 4.08; found: C 52.58, H 5.91, N 4.10.

Complex 7c: Complex **7c** was synthesized according to the procedure described for **3b** using [Pd(η^1,η^2-C$_8$H$_{12}$OMe)Cl]$_2$ (100 mg, 0.36 mmol), N,N'-(1,2-dimethyl-1,2-ethanediylidene)bis(2,6-dimethyl)benzenamine (108 mg, 0.37 mmol), and NaB[3,5-(CF$_3$)$_2$C$_6$H$_3$]$_4$ (328 mg, 0.37 mmol). It was isolated as an orange powder (448 mg, 0.32 mmol; yield 89%). ^{1}H NMR (400 MHz, CD$_2$Cl$_2$, −40°C): δ = 7.73 (m, 8H; o-H), 7.55 (s, 4H; p-H), 7.28–7.14 (br, 6H; H11, H11a, H12, H15, H15a, and H16), 5.32 (m, 1H; H1), 4.71 (m, 1H; H2), 2.96 (m, 1H; H5), 2.64 (m, 1H; H3), 2.47 (m, 1H; H3'), 2.38 (s, 3H; OMe), 2.27 (s, 3H; H19 or H20), 2.22 (s, 6H; H21 and H23), 2.19 (s, 3H; H22), 2.15 (3H; H20 or H19), 2.11 (brm, 3H; H7, H8 and H8'), 2.07 (s, 3H; H24), 1.98 (m, 1H; H6), 1.84 (m, 2H; H4 and H4'), 1.44 ppm (m, 1H; H7'); ^{13}C{^{1}H} NMR (100 MHz, CD$_2$Cl$_2$, −40°C): δ = 179.8 (s; C17 or C18), 174.2 (s; C18 or C17), 162.0 (q, $^1J_{C,B}$ = 49.5 Hz; C-ipso), 142.6 (s; C13 or C9), 141.6 (s; C9 or C13), 135.1 (s, o-C), 118.0 (s, p-C), 129.1 (q, $^2J_{C,F}$ = 29.2 Hz; C-CF$_3$), 124.9 (q, $^1J_{C,F}$ = 272.3 Hz; CF$_3$), 130.1, 129.74, 129.68, 129.5, 128.6, 128.5, 128.0, 127.2, 126.8, 126.5 (C10, C10a, C11, C11a, C12, C14, C14a, C15, C15a, C16), 113.2 (s; C1), 110.5 (s; C2), 81.9 (s; C5), 56.6 (s; C6), 55.9 (s, OMe), 33.9 (s; C7), 31.5 (s; C4), 29.8 (s; C3), 26.5 (s; C8), 20.5 (s; C19 or C20), 19.9 (C20 or C19), 18.6 (s; C22), 18.4 (s; C23), 18.3 (s; C21), 18.0 ppm (s; C24); ^{19}F NMR (376 MHz, CD$_2$Cl$_2$, −40°C): δ = −63.0 ppm (s, 24F; CF$_3$); elemental analysis calcd (%) for C$_{61}$H$_{51}$BF$_{24}$N$_2$OPd (1401.3): C 52.67, H 3.70, N 2.01; found: C 52.58, H 3.91, N 2.06.

Complex 10: Complex **10** was synthesized according to the procedure described for **3b** using [Pd(η^1,η^2-C$_8$H$_{12}$OMe)Cl]$_2$ (100 mg, 0.36 mmol), N,N'-(1,2-dimethyl-1,2-ethanediylidene)bis(2,4,6-trifluoro)benzenamine (127 mg, 0.37 mmol), and AgBF$_4$ (28 mg, 0.38 mmol). It was isolated as a yellow powder (146 mg, 0.21 mmol; yield 60%). ^{1}H NMR (400 MHz,

CD$_2$Cl$_2$, −69°C): δ = 7.03 (m, 5H; H15a, H15, H11a, H11), 5.71 (m, 1H; H1), 4.90 (m, 1H; H2), 3.21 (m, 1H; H5), 2.70 (s, 3H; OMe), 2.60 (s, 3H; H20 or H19), 2.49 (m, 2H; H3 and H3'), 2.47 (s, 3H; H19 or H20), 2.17 (m, 4H; H7 or H7', H8, H8', H6), 1.85 (m, 2H; H4 and H4'), 1.88 ppm (m, 1H; H7'or H7); ^{19}F NMR (376 MHz, CD$_2$Cl$_2$, −69°C): δ = −106.1 (s, 1F; F16 or F12), −106.7 (s, 1F; F12 or F16), −115.1 (s, 1F; F14a or F10), −115.4 (s, 1F; F10a or F14), −116.7 (s, 1F; F14 or F10a), −117.1 (s, 1F; F10 or F14a), −152.09 (s, 4F; ^{10}BF$_4$$^-$), −152.15 ppm (s, 4F; ^{11}BF$_4$$^-$); elemental analysis calcd (%) for C$_{25}$H$_{25}$BF$_{10}$N$_2$OPd (676.7): C 44.37, H 3.72, N 4.14; found: C 44.83, H 3.96, N 3.79.

Complex 11: Complex **11** was synthesized according to a literature procedure[23] from [Pd(η^1,η^2-C$_8$H$_{12}$OMe)Cl]$_2$ (100 mg, 0.18 mmol), the N,N'-(1,2-dimethyl-1,2-ethanediylidene)bis(2-methyl)benzenamine (95 mg, 0.36 mmol), and NH$_4$PF$_6$ (150 mg). It was isolated as a yellow powder (179 mg, 0.27 mmol; yield 75%). A complete NMR characterization was only possible for the major isomer c. ^{1}H NMR (400 MHz, CD$_2$Cl$_2$, −56°C): δ = 7.40–7.33 (m, 4H; H11a, H11, H15a, and H15), 7.26 (m, 2H; H16 and H12), 7.12 (m, 1H; H10a), 6.95 (m, 1H; H14a), 5.14 (br, 3H; H19), 4.99 (br, 1H; H2), 3.04 (m, 1H; H5), 2.52 (br, 2H; H3 and H3'), 2.33 (s, 3H; OMe), 2.32 (s, 3H; H23), 2.29 (s, 6H; H19 and H21), 2.18 (s, 3H; H20), 2.08 (br, 3H; H8, H8', and H7), 1.92 (br, 1H; H6), 1.75 (br, 2H; H4 and H4'), 1.41 ppm (br, 1H; H7'); ^{13}C{^{1}H} NMR (100 MHz, CD$_2$Cl$_2$, −56°C): δ = 180.3 (s; C17 or C18), 174.6 (s; C18 or C17), 144.6 (s; C9 or C13), 143.4 (s; C13 or C9), 131.8, 131.7, 131.6, 129.7, 128.4, 128.2, 128.0, 127.8 (s; C11a, C12, C11, C10, C15a, C16, C15, C14), 120.7 (s; C10a), 120.2 (s; C14a), 111.3 (s; C2), 109.1 (s; C1), 81.1 (s; C5), 55.6 (s, OMe), 54.3 (s; C6), 34.1 (s; C7), 31.5 (s; C4), 29.0 (s; C3), 26.4 (s; C8), 21.0 (s; C19), 20.0 (s; C20), 18.5 (s; C23), 18.4 ppm (s; C21); ^{19}F NMR (376 MHz, CD$_2$Cl$_2$, −56°C): δ = −72.57 ppm (d, $^1J_{F,P}$ = 711.8 Hz, 6F; PF$_6$$^-$); elemental analysis calcd (%) for C$_{27}$H$_{35}$F$_6$N$_2$OPPd: (655) C 49.51, H 5.39, N 4.28; found: C 49.53, H 5.45, N 4.29.

Complex 12a: Complex **12a** was synthesized according to a literature procedure[23] from [Pd(η^1,η^2-C$_8$H$_{12}$OMe)Cl]$_2$ (100 mg, 0.18 mmol), N,N'-(1,2-dimethyl-1,2-ethanediylidene)bis(2-ethyl)benzenamine (105 mg, 0.36 mmol), and NH$_4$PF$_6$ (150 mg). It was isolated as a yellow powder (184 mg, 0.27 mmol; yield 75%). A complete NMR characterization was only possible for the major isomer c. ^{1}H NMR (400 MHz, CD$_2$Cl$_2$, −56°C): δ = 7.47–7.28 (m, 6H; H11a, H12, H11, H15a, H16, H15), 7.14 (m, 1H; H10a), 6.97 (m, 1H; H14a), 5.07 (m, 1H; H1), 4.99 (m, 1H; H2), 3.05 (m, 1H; H5), 2.71 (m, 2H; H23), 2.67 (m, 2H; H21), 2.55 (m, 1H; H3), 2.45 (m, 1H; H3'), 2.36 (s, 3H; OMe), 2.32 (s, 3H; H19), 2.21 (s, 3H; H20), 2.10 (m, 3H; H8, H8', and H7), 1.88 (m, 1H; H6), 1.74 (m, 2H; H4 and H4'), 1.40 (m, 1H; H7'), 1.27 (m, 3H; H27), 1.23 ppm (m, 3H; H25); ^{13}C{^{1}H} NMR (100 MHz, CD$_2$Cl$_2$, −56°C): δ = 179.9 (s; C17 or C18), 174.3 (s; C18 or C17), 144.1 (s; C9 or C13), 142.9 (s; C13 or C9), 135.1 (s; C10 or C14), 133.9 (s; C14 or C10), 130.0, 129.6, 128.5, 128.4, 128.0, 127.8 (s; C11a, C12, C11, C15a, C16, C15), 121.0 (s; C10a), 120.5 (s; C14a), 111.2 (s; C2), 108.8 (s; C1), 81.0 (s; C5), 55.6 (s, OMe), 54.7 (s; C6), 33.8 (s; C7), 31.4 (s; C4), 28.8 (s; C3), 26.3 (s; C8), 25.6 (s; C23), 25.5 (s; C21), 21.2 (s; C19), 20.6 (s; C20), 15.0 (s; C25), 14.1 ppm (s; C27); ^{19}F NMR (376 MHz, CD$_2$Cl$_2$, −56°C): δ = −72.52 ppm (d, $^1J_{F,P}$ = 715.5 Hz, 6F; PF$_6$$^-$); elemental analysis calcd (%) for C$_{29}$H$_{39}$F$_6$N$_2$OPPd (683): C 51.00, H 5.76, N 4.10; found: C 51.53, H 5.79, N 4.11.

Complex 12b: Complex **12b** was synthesized according to the procedure described for **3b** using [Pd(η^1,η^2-C$_8$H$_{12}$OMe)Cl]$_2$ (100 mg, 0.18 mmol), N,N'-(1,2-ethanediylidene)bis(2-ethyl)benzenamine (105 mg, 0.37 mmol), and AgCF$_3$SO$_3$ (98 mg, 0.38 mmol). It was isolated as a yellow powder (223 mg, 0.33 mmol; yield 90%). A complete NMR characterization was only possible for the major isomer c. ^{1}H NMR (400 MHz, CD$_2$Cl$_2$, −56°C): δ = 7.47–7.27 (m, 6H; H11a, H12, H11, H15a, H16, H15), 7.23 (d, 1H; H10a), 7.08 (m, 1H; H14a), 5.08 (m, 1H; H1), 5.00 (m, 1H; H2), 3.06 (m, 1H; H5), 2.72–2.60 (m, 4H; H23 and H21), 2.48 (m, 2H; H3, H3'), 2.37 (s, 3H; OMe), 2.35 (s, 3H; H19), 2.24 (s, 3H; H20), 2.06 (m, 3H; H8, H8' and H7), 1.88 (m, 1H; H6), 1.75 (m, 2H; H4 and H4'), 1.40 (m, 1H; H7'), 1.27 (m, 3H; H27), 1.23 ppm (m, 3H; H25); ^{13}C{^{1}H} NMR (100 MHz, CD$_2$Cl$_2$, −56°C): δ = 180.3 (s; C17 or C18), 174.7 (s; C18 or C17), 144.0 (s; C9 or C13), 143.0 (s; C13 or C9), 135.0 (s; C10 or C14), 133.7 (s; C14 or C10), 129.9, 129.6, 128.4, 128.2, 128.1, 127.8 (s; C11a,

C12, C11, C15a, C16, C15), 121.1 (q, $^1J_{C,F} = 320.6$ Hz; CF$_3$SO$_3$), 121.2 (s; C10a), 120.7 (s; C14a), 111.1 (s; C2), 108.8 (s; C1), 81.0 (s; C5), 55.7 (s, OMe), 54.8 (s; C6), 33.8 (s; C7), 31.3 (s; C4), 28.8 (s; C3), 26.3 (s; C8), 25.6 (s; C23), 25.5 (s; C21), 21.5 (s; C19), 20.4 (s; C20), 15.0 (s; C25), 14.2 ppm (s; C27); elemental analysis calcd (%) for C$_{30}$H$_{39}$F$_9$N$_2$O$_4$PdS (801.1): C 55.51, H 6.09 N 4.32; found: C 55.70, H 6.12, N 4.39.

Complex 12c: Complex **12c** was synthesized according to the procedure described for **3b** using [Pd(η^1,η^2-C$_8$H$_{12}$OMe)Cl]$_2$ (100 mg, 0.36 mmol), N,N′-(1,2-dimethyl-1,2-ethanediylidene)bis(2-ethyl)benzenamine (105 mg, 0.37 mmol), and NaB[3,5-(CF$_3$)$_2$C$_6$H$_3$]$_4$ (337 mg, 0.38 mmol). It was isolated as a yellow powder (449 mg, 0.32 mmol; yield 89%). A complete NMR characterization was only possible for the major isomer c. ^{1}H NMR (400 MHz, CD$_2$Cl$_2$, −56°C): $\delta = 7.48$–7.30 (br, 6H; H15, H11, H11a, H15a, H16), 6.92 (m, 1H; H10a), 6.73 (m, 1H; H14a), 5.22 (m, 1H; H1), 4.96 (m, 1H; H2), 3.00 (m, 1H; H5), 2.65–2.58 (m, 4H; H23, H21), 2.54 (m, 1H; H3 or H3′), 2.43 (m, 1H; H3′ or H3), 2.36 (s, 3H; OMe), 2.32 (s, 3H; H19), 2.22 (s, 3H; H20), 2.09 (m, 3H; H8, H8′ and H7), 1.99 (m, 1H; H6), 1.77 (m, 2H; H4 and H4′), 1.40 (m, 1H; H7′), 1.28 (m, 3H; H27), 1.21 ppm (m, 3H; H25); ^{13}C{^{1}H} NMR (100 MHz, CD$_2$Cl$_2$, −56°C): $\delta = 179.3$ (s; C17 or C18), 173.8 (s; C18 or C17), 162.18 (q, $^1J_{C,B} = 49.6$ Hz; BArF-C$_{ipso}$), 143.6 (s; C9 or C13), 142.4 (s; C13 or C9), 135.1 (s, BArF-C$_{ortho}$), 134.9 (s; C10 or C14), 133.5 (s; C14 or C10), 130.1 (s; C15), 129.6 (s; C11), 129.1 (q, $^1J_{C,F} = 31.7$, BArF-C$_{meta}$) 128.5, 128.4, 128.1, 127.9 (s; C11a, C15a, C16, C12), 124.9 (q, $^1J_{C,F} = 272.5$; BArF-CF$_3$), 120.8 (s; C10a), 120.1 (s; C14a), 111.1 (s; C2), 109.0 (s; C1), 81.0 (s; C5), 55.8 (s, OMe), 54.7 (s; C6), 34.3 (s; C7), 31.3 (s; C4), 29.2 (s; C3), 26.3 (s; C8), 25.5 (s; C23), 25.4 (s; C21), 21.6 (s; C19), 20.6 (s; C20), 14.8 (s; C25), 14.0 ppm (s; C27); elemental analysis calcd (%) for C$_{61}$H$_{51}$BF$_{24}$N$_2$OPd (1401.3): C 52.67, H 3.70, N 2.01; found: C 52.88, H 3.73, N 2.05.

Complex 13: Complex **13** was synthesized according to a literature procedure[23] from [Pd(η^1,η^2-C$_8$H$_{12}$OMe)Cl]$_2$ (100 mg, 0.18 mmol), N,N′-(1,2-dimethyl-1,2-ethanediylidene)bis(2-isopropyl)benzenamine ligand (116 mg, 0.36 mmol), and NH$_4$PF$_6$ (150 mg). It was isolated as a yellow powder (194 mg, 0.27 mmol; yield 75%). A complete NMR characterization was only possible for the major isomer c. ^{1}H NMR (400 MHz, CD$_2$Cl$_2$, −29°C): $\delta = 7.50$ (d, $^3J(H,H) = 7.6$ Hz, 1H; H11), 7.47 (d, $^3J(H,H) = 7.3$ Hz, 1H; H15), 7.43–7.32 (m, 4H; H11a, H15a, H16, H12), 7,14 (d, ^3J-(H,H) = 7.7 Hz, 1H; H10a), 6.97 (d, $^3J(H,H) = 7.4$ Hz, 1H; H14a), 5.11 (m, 1H; H2), 5.05 (m, 1H; H1), 3.18 (sept, $^3J_{H,H} = 6.7$ Hz, 1H; H23), 3.05 (m, 2H; H21 and H5), 2.53 (m, 2H; H3 and H3′), 2.35 (s, 3H; H19), 2.33 (s, 3H; OMe), 2.24 (s, 3H; H$_2$O), 2.07 (m, 3H; H8, H8′ and H7), 1.93 (m, 1H; H6), 1.75 (m, 2H; H4 and H4′), 1.49 (d, $^3J_{H,H} = 6.7$ Hz, 3H; H27f), 1.42 (d, $^3J_{H,H} = 6.7$ Hz, 3H; H25f), 1,39 (m, 1H; H7′), 1.11 (d, ^3J-(H,H) = 6.7 Hz, 3H; H25b), 1.08 ppm (d, $^3J(H,H) = 6.7$ Hz, 3H; H27b); ^{13}C{^{1}H} NMR (100 MHz, CD$_2$Cl$_2$, −29°C): $\delta = 179.7$ (s; C17 or C18), 174.2 (s; C18 or C17), 143.2 (s; C9 or C13), 142.1 (s; C13 or C9), 139.6 (s; C10 or C14), 138.4 (s; C14 or C10), 128.8, 128.4, 128.3, 127.9 (s; C11a, C15a, C16, C12), 126.9 (s; C15), 126.8 (s; C11), 121.4 (s; C10a), 120.8 (s; C14a), 111.7 (s; C2), 108.1 (s; C1), 81.0 (s; C5), 55.5 (s, OMe), 54.9 (s; C6), 33.4 (s; C7), 31.4 (s; C4), 30.0 (s; C21), 29.9 (s; C23), 28.8 (s; C3), 26.2 (s; C8), 24.8 (s; C27b), 24.3 (s; C25b), 22.2 (s; C25f), 22.1 (s; C27f), 21.4 (s; C19), 20.4 ppm (s; C20); ^{19}F NMR (376 MHz, CD$_2$Cl$_2$, −29°C): $\delta = -72.47$ ppm (d, $^1J_{F,P} = 713.0$ Hz, 6F; PF$_6^-$); elemental analysis calcd (%) for C$_{31}$H$_{43}$F$_6$N$_2$OPPd (711.1): C 52.36, H 6.10, N 3.94; found: C 52.46, H 6.16, N 3.95.

Complex 14: Complex **14** was synthesized according to the procedure described for **3b** using [Pd(η^1,η^2-C$_8$H$_{12}$OMe)Cl]$_2$ (100 mg, 0.36 mmol), N,N′-(1,2-dimethyl-1,2-ethanediylidene)bis(2-trifluoromethyl)benzenamine (138 mg, 0.37 mmol), and AgBF$_4$ (74 mg, 0.38 mmol). It was isolated as a yellow powder (226 mg, 0.32 mmol; yield 85%); elemental analysis calcd (%) for C$_{27}$H$_{29}$BF$_{10}$N$_2$OPd (704.8): C 46.02 H 4.15 N 3.97; found: C 46.15, H 4.30, N 4.02. Major isomer c: ^{1}H NMR (400 MHz, CD$_2$Cl$_2$, −77°C): $\delta = 7.83$–7.73 (m, 4H; H11a, H11, H15a, and H15), 7.59 (br d, 1H; H10a), 7.50–7.45 (m, 2H; H12 and H16), 7.38 (m, 1H; H14a), 5.08 (m, 2H; H1 and H2), 3.15 (m, 1H; H5), 2.75 (m, 1H; H3), 2.47 (m, 4H; OMe and H3′), 2.28 (s, 3H; H19), 2.15 (s, 3H; H20), 1.98 (m, 3H; H8, H8′, and H6), 1.78 (m, 2H; H4 and H4′), 1.21 ppm (m, 2H; H7 and H7′);

^{19}F NMR (376 MHz, CD$_2$Cl$_2$, −77°C): $\delta = -61.68$ (s, 3F; CF$_3$-23), −62.62 (s, 3F; CF$_3$-21), −149.81 (s, 4F; ^{10}BF$_4$), −149.87 ppm (s, 4F; ^{11}BF$_4$). Second most abundant isomer d: ^{1}H NMR (400 MHz, CD$_2$Cl$_2$, −77°C): δ 7.83–7.73 (m, 4H; H11, H11a, H15, and H15a), 7.59 (br d, 1H; H10), 7.50–7.45 (m, 2H; H12 and H16), 7.38 (m, 1H; H14), 5.56 (m, 1H; H1), 4.55 (m, 1H; H2), 3.07 (m, 1H; H5), 2.47 (s, 3H; OMe), 2.30 (m, 2H; H3 and H3′), 2.28 (s, 3H; H19), 2.17 (m, 2H; H8 and H8′), 2.15 (s, 3H; H20), 2.12 (m, 1H; H6), 1.79 (m, 1H; H4), 1.66 (m, 1H; H4′), 1.21 ppm (m, 2H; H7 and H7′); ^{19}F NMR (376 MHz, CD$_2$Cl$_2$, −77°C): $\delta = -61.57$ (s, 3F; CF$_3$-22), −62.48 (s, 3F; CF$_3$-24), −149.81 (s, 4F; ^{10}BF$_4$), −149.87 ppm (s, 4F; ^{11}BF$_4$).

Complex 15: Complex **15** was synthesized according to the procedure described for **3b** using [Pd(η^1,η^2-C$_8$H$_{12}$OMe)Cl]$_2$ (100 mg, 0.36 mmol), N,N′-(1,2-dimethyl-1,2-ethanediylidene)bis(2,4-difluoro)benzenamine (114 mg, 0.37 mmol), and AgBF$_4$ (74 mg, 0.38 mmol). It was isolated as a yellow powder (90 mg, 0.14 mmol; yield 40%). In the following data, A, B, C, and D indicate the different isomers in order of abundance. ^{1}H NMR (400 MHz, CD$_2$Cl$_2$, −69°C): $\delta = 7.63$–6.70 (m, 6H; aromatic protons), 5.63–4.75 ppm (m, 2H; olefinic protons), 3.25–1.25 ppm (m, 21H; aliphatic protons); ^{19}F NMR (376 MHz, CD$_2$Cl$_2$, −69°C): $\delta = -110.72$, −111.40, −119.19, −119.52 (m, 4F; isomer A), −110.64, −111.00, −119.96, −120.86 (m, 4F; isomer B), −109.79, −110.27, −118.19, −119.01 (m, 4F; isomer C), −110.00, −110.62, −118.51, −118.51 (m, 4F; isomer D), −150.46 (s, 4F; ^{10}BF$_4^-$), −150.51 ppm (s, 4F; ^{11}BF$_4^-$); elemental analysis calcd (%) for C$_{25}$H$_{27}$BF$_8$N$_2$OPd (640.7): C 46.87, H 4.25, N 4.37; found: C 46.94, H 4.38, N 4.40.

Complex 16: Complex **16** was synthesized according to the procedure described for **3b** using [Pd(η^1,η^2-C$_8$H$_{12}$OMe)Cl]$_2$ (100 mg, 0.36 mmol), N,N′-(1,2-dimethyl-1,2-ethanediylidene)bis(3,4-difluoro)benzenamine (114 mg, 0.37 mmol), and AgBF$_4$ (74 mg, 0.38 mmol). It was isolated as a yellow powder (115 mg, 0.18 mmol; yield 50%). ^{1}H NMR (400 MHz, CD$_2$Cl$_2$, −69°C): $\delta = 7.50$–6.25 (m, 6H; aromatic protons), 5.50–4.75 (m, 2H; olefinic protons), 3.25–1.25 ppm (m, 21H; aliphatic protons); ^{19}F NMR (376 MHz, CD$_2$Cl$_2$, −29°C): $\delta = -133.5$–141.0 (4F; fluorine atoms of organometallic fragment), −150.03 (s, 4F; ^{10}BF$_4^-$), −150.09 ppm (s, 4F; ^{11}BF$_4^-$); elemental analysis calcd (%) for C$_{25}$H$_{27}$BF$_8$N$_2$OPd (640.7): C 46.87, H 4.25, N 4.37; found: C 47.35, H 4.51, N 4.39.

CO/p-Methylstyrene copolymerization: In a typical copolymerization reaction the Pd^{II} complex (0.14 mmol) was dissolved in dichloromethane (5 mL) at 17°C under nitrogen, then p-methylstyrene (5.5 mL, 42 mmol) was added (olefin/palladium molar ratio: 300:1). The resulting solution was transferred into a thermostatted Schlenk flask equipped with a carbon monoxide gas line and a tank for the CO. The solution was allowed to react for 51 h at 17°C. The resulting gray polymer was precipitated with methanol and washed with methanol. To remove metallic palladium, the polymer was redissolved in chloroform, filtered through Celite, precipitated with methanol, washed with methanol, and dried under vacuum. When mixtures of copolymer and poly(p-methylstyrene) were obtained from the reaction, diethyl ether was added to the mixture in order to extract the homopolymer. The resulting suspension was stirred vigorously for several hours and the ether solution was decanted off from the powder. The ^{1}H and ^{13}C NMR spectroscopic data were consistent with the isolation of atactic polyketones when catalysts **1–4**, **12c**, and **15** were used. IR (CHCl$_3$): $\tilde{\nu} = 1710$ cm^{-1}(CO); ^{1}H NMR (400 MHz, CDCl$_3$, 20°C): $\delta = 7.01$–6.54 (br m, 4H; Ph), 3.97 (br m, 1H; CHCH$_2$), 3.09 (br m, 1H; CHCH_2), 2.58 (br m, 1H; CHCH_2), 2.24 ppm (br, 3H; PhCH_3); ^{13}C{^{1}H} NMR (100 MHz, (CF$_3$)$_2$CHOH/CDCl$_3$ 1/1 (v/v), 35°C): $\delta = 210.90$–210.12 (br, CO), 138.4–138.2 (br, Ph-C$_p$), 133.6–132.2 (br, Ph-C$_{ipso}$), 130.1 (s, Ph-C$_o$), 128.1 (s, Ph-C$_m$), 53.6–53.3 (br, CH-CH$_2$), 44.8–42.9 (br, CH-CH$_2$), 20.4 ppm (s, Ph-CH$_3$). The ^{1}H and ^{13}C NMR spectroscopic data were consistent with the isolation of predominantly isotactic polyketones when catalysts **5–7**, **11–12b**, and **13** were used. ^{1}H NMR (400 MHz, CDCl$_3$, 20°C): $\delta = 7.01$ (br m, 2H; Ph), 6.87 (br m, 2H; Ph), 3.88 (br m, 1H; CHCH$_2$), 3.13 (br m, 1H; CHCH_2), 2.58 (br m, 1H; CHCH_2), 2.29 (br, 3H; PhCH_3); ^{13}C{^{1}H} NMR (100 MHz, (CF$_3$)$_2$CHOH/CDCl$_3$ 1/1 (v/v), 35°C): $\delta = 210.5$ (s; CO), 138.2 (s; Ph-C$_p$), 133.6 (s; Ph-C$_{ipso}$), 130.0 (s; Ph-C$_o$), 128.1 (s; Ph-C$_m$), 52.8 (s; CHCH$_2$), 44.9 (s; CHCH_2), 20.5 ppm (s, PhCH_3). [α]$_{589}^{25} < 1°$ (c = 1.67 mg mL^{-1}, CH$_2$Cl$_2$); ele-

mental analysis calcd (%) for $(C_{10}H_{10}O)_n$: C 82.16, H 6.89; found: C 82.50, H 7.21.

X-ray crystallographic structure determination for 3a, 5a, 7a, and 13: Single crystals suitable for X-ray diffraction were obtained by slow diffusion of hexane into a dichloromethane solution of the complex at −30°C. Diffraction intensities were collected at room temperature with an XCALIBUR (CCDareal) diffractometer using graphite-monochromated Mo$_{K\alpha}$ radiation ($\lambda = 0.71073$ Å), ωp scans, and the frame data were acquired with the CRYSALIS (CCD 170) software. The crystal-to-detector distance was 65.77 mm. The structure was solved by direct methods and refined against $|F|^2$. Crystallographic data are listed in Table 2. The frames

Table 2. Crystallographic data for **3a**, **5a**, **7a**, and **13**.

	3a	5a·CH₂Cl₂	7a	13
formula	$C_{26}H_{14}F_8N_2OPPd$	$C_{28}H_{37}Cl_2F_6N_2OPPd$	$C_{29}H_{39}F_6N_2OPPd$	$C_{31}H_{43}F_6N_2OPPd$
M	659.78	739.87	682.99	711.04
T [K]	295	295	295	296
color	yellow	orange	orange	yellow
cryst. syst	monoclinic	triclinic	monoclinic	monoclinic
space group	$C2/m$	$P\bar{1}$	$P2_1/c$	$C2/c$
a [Å]	26.598(5)	11.030(5)	11.8320(10)	39.281(5)
b [Å]	8.051(5)	12.139(5)	23.4420(10)	10.221(5)
c [Å]	18.554(5)	12.790(5)	12.4730(10)	16.654(5)
α [°]	90.00	91.365(5)	90.00	90.00
β [°]	133.047(5)	92.987(5)	116.420(10)	104.96(5)
γ [°]	2904(2)	1632.4(12)	3098.3(4)	6460(4)
V [Å³]	2904(2)	1632.4(12)	3098.3(4)	6460(4)
Z	4	2	4	8
ρ_{calcd} [g cm⁻³]	1.507	1.505	1.464	1.462
R_{int}	0.0857	0.0594	0.0607	0.0518
GOF	1.075	0.977	1.086	1.099

were processed using the CRYSALIS (RED 170) software to give the *hkl* file corrected for scan speed, background, and Lorentz and polarization affects. Standard reflections, measured periodically, showed no apparent variation in intensity during data collection and so no correction for crystal decomposition was necessary. The data were corrected for absorption using the Multiscan[65] program. The structure was solved by direct methods using the SIR-97[66] program and refined by full-matrix least-squares methods on F^2 using SHELXL-97[67] WinGX[68] version. All non-hydrogen atoms were refined anisotropically. The hydrogen atoms were added at calculated positions and refined using a riding model. Complex **5a** includes one molecule of dichloromethane in the asymmetric unit of the crystallographic cell.

Analogous to other similar complexes,[54] the C(6)−C(5)−OMe moiety of the methoxycyclooctenyl ligand is disordered over two enantiomeric orientations in complexes **3a**, **5a**, and **7a**. Refinement of the relative contribution to each orientation converged to an occupancy factor ratio of 50:50 for **3a**, 75:25 for **5a**, and 65:35 for **7a**.

Acknowledgments

[1] V. C. Gibson, S. K. Spitzmesser, *Chem. Rev.* **2003**, *103*, 283.
[2] J.-N. Pedeutour, K. Radhakrishnan, H. Cramail, A. Deffieux, *Macromol. Rapid Commun.* **2001**, *22*, 1095.
[3] *Chem. Rev.* **2000**, *100* (special issue on "Frontiers in Metal-Catalyzed Polymerization"; Ed.: J. A. Gladysz).
[4] *Top. Catal.* **1999**, vol. 15 (Eds.: T. J. Marks, J. C. Stevens), and references therein.
[5] A. Sen in *Catalytic Synthesis of Carbon Monoxide/Alkenes Copolymers and Cooligomers* (Ed.: A. Sen), Kluwer Academic, Dordrecht, **2003**, pp. 1–7.
[6] C. Bianchini, A. Meli, *Coord. Chem. Rev.* **2002**, *225*, 35.
[7] J. Durand, B. Milani, *Coord. Chem. Rev.* **2006**, *250*, 542.
[8] E. Y.-X. Chen, T. J. Marks, *Chem. Rev.* **2000**, *100*, 1391.
[9] M. Bochmann, *J. Organomet. Chem.* **2004**, *689*, 3982.
[10] A. Macchioni, *Chem. Rev.* **2005**, *105*, 2039.
[11] E. Drent, P. H. M. Budzelaar, *Chem. Rev.* **1996**, *96*, 663.
[12] G. Consiglio in *Late Transition Metal Polymerization Catalysis* (Eds.: B. Rieger, L. Saunders Baugh, S. Kacker, S. Striegler), Wiley, **2003**, p. 279.
[13] A. Macchioni, G. Bellachioma, G. Cardaci, M. Travaglia, C. Zuccaccia, B. Milani, G. Corso, E. Zangrando, G. Mestroni, C. Carfagna, M. Formica, *Organometallics* **1999**, *18*, 3061.
[14] A. Gsponer, B. Milani, G. Consiglio, *Helv. Chim. Acta* **2002**, *85*, 4074.
[15] D. Sirbu, G. Consiglio, B. Milani, P. G. A. Kumar, P. S. Pregosin, S. Gischig, *J. Organomet. Chem.* **2005**, *690*, 2254.
[16] A. Scarel, J. Durand, D. Franchi, E. Zangrando, G. Mestroni, C. Carfagna, L. Mosca, R. Seraglia, G. Consiglio, B. Milani, *Chem. Eur. J.* **2005**, *11*, 6014.
[17] J. Brownie, M. C. Baird, L. N. Zakharov, A. L. Rheingold, *Organometallics* **2003**, *22*, 33.
[18] S. D. Ittel, L. Johnson, M. Brookhart, *Chem. Rev.* **2000**, *100*, 1169.
[19] M. D. Leatherman, M. Brookhart, *Macromolecules* **2001**, *34*, 2748.
[20] B. Binotti, C. Carfagna, C. Zuccaccia, A. Macchioni, *Chem. Commun.* **2005**, 92.
[21] S. D. Arthur, M. S. Brookhart, L. K. Johnson, C. K. Killian, E. F. McCord, S. J. McLain, U.S. Patent 5891963, April 6, **1996**.
[22] L. K. Johnson, C. K. Killian, M. Brookhart, *J. Am. Chem. Soc.* **1995**, *117*, 6414.
[23] G. Bellachioma, B. Binotti, G. Cardaci, C. Carfagna, A. Macchioni, S. Sabatini, C. Zuccaccia, *Inorg. Chim. Acta* **2002**, *350*, 44.
[24] L. Deng, T. K. Woo, L. Cavallo, P. M. Margl, T. Ziegler, *J. Am. Chem. Soc.* **1997**, *119*, 6177.
[25] D. J. Tempel, L. K. Johnson, R. L. Huff, P. S. White, M. Brookhart, *J. Am. Chem. Soc.* **2000**, *122*, 6686.
[26] T. K. Woo, P. E. Blöchl, T. Ziegler, *J. Phys. Chem. A* **2000**, *104*, 121.
[27] P. Margl, T. Ziegler, *Organometallics* **1996**, *15*, 5519.
[28] T. Schleis, T. P. Spaniol, J. Okuda, J. Heinemann, R. Mülhaupt, *J. Organomet. Chem.* **1998**, *569*, 159.
[29] A. Michalak, T. Ziegler, *Organometallics* **2000**, *19*, 1850.
[30] C. Zuccaccia, A. Macchioni, I. Orabona, F. Ruffo, *Organometallics* **1999**, *18*, 4367.
[31] A. Macchioni, A. Magistrato, I. Orabona, F. Ruffo, U. Röthlisberger, C. Zuccaccia, *New J. Chem.* **2003**, *27*, 455.
[32] A. Macchioni, *Eur. J. Inorg. Chem.* **2003**, 195, and references therein.
[33] This was evaluated from the intensities of the ¹³C NMR C5-carbon atom resonances, while for **14** it was evaluated from the intensities of the CF₃-fluorine resonance, which appears at around $\delta = -60$ ppm in the ¹⁹F NMR spectrum.
[34] T. Schleis, T. P. Spaniol, J. Okuda, J. Heinemann, R. Mülhaupt, *J. Organomet. Chem.* **1998**, *569*, 159.
[35] D. P. Gates, S. A. Svejda, E. Oñate, C. M. Killian, L. K. Johnson, P. S. White, M. Brookhart, *Macromolecules* **2000**, *33*, 2320.

[36] R. Van Belzen, R. A. Klein, H. Kooijman, N. Veldman, A. L. Spek, C. Elsevier, *Organometallics* **1998**, *17*, 1812.

[37] M. Fusto, F. Giordano, I. Orabona, F. Ruffo, *Organometallics* **1997**, *16*, 5981.

[38] P. Ganis, I. Orabona, F. Ruffo, A. Vitagliano, *Organometallics* **1998**, *17*, 2646.

[39] K. Yang, R. J. Lachicotte, R. Eisenberg, *Organometallics* **1998**, *17*, 5102.

[40] K. Yang, R. J. Lachicotte, R. Eisenberg, *Organometallics* **1997**, *16*, 5234.

[41] S. H. Strauss, *Chem. Rev.* **1993**, *93*, 927.

[42] Semi-quantitative monitoring of the CO uptake indicates a particularly long induction period as the prevalent reason for the observed low activity of precatalyst **7b** compared to the others.

[43] A. Gsponer, G. Consiglio, *Helv. Chim. Acta* **2003**, *86*, 2170.

[44] M. Sperrle, A. Aeby, G. Consiglio, A. Pfaltz, *Helv. Chim. Acta* **1996**, *79*, 1387.

[45] A. Aeby, G. Consiglio, *Inorg. Chim. Acta* **1999**, *296*, 45.

[46] A. Aeby, A. Gsponer, G. Consiglio, *J. Am. Chem. Soc.* **1998**, *120*, 11000.

[47] H. A. Zhong, J. A. Labinger, J. E. Bercaw, *J. Am. Chem. Soc.* **2002**, *124*, 1378.

[48] D. Pappalardo, M. Mazzeo, C. Pellecchia, *Macromol. Rapid Commun.* **1997**, *18*, 1017.

[49] R. D. J. Froese, D. G. Musaev, K. Morokuma, *J. Am. Chem. Soc.* **1998**, *120*, 1581.

[50] The narrow molecular-weight distributions of polyketones produced by *ortho*-monosubstituted catalysts (Table 2, entries 17–22) agrees with the presence of a single active species. Brookhart has found polydispersities of up to 4.4 in polyethylene produced by catalysts bearing analogous mono *ortho*-substituted α-diimine ligands, which were attributed to the presence in solution of species of both symmetries (C_2 and C_s). See ref. [35].

[51] D. Pappalardo, M. Mazzeo, S. Antinucci, C. Pellecchia, *Macromolecules* **2000**, *33*, 9483.

[52] C. Propeney, Z. Guan, *Organometallics* **2005**, *24*, 1145.

[53] S. A. Svejda, M. Brookhart, *Organometallics* **1999**, *18*, 65.

[54] B. Binotti, G. Bellachioma, C. Cardaci, A. Macchioni, C. Zuccaccia, E. Foresti, P. Sabatino, *Organometallics* **2002**, *21*, 346.

[55] B. Binotti, C. Carfagna, E. Foresti, A. Macchioni, P. Sabatino, C. Zuccaccia, D. Zuccaccia, *J. Organomet. Chem.* **2004**, *689*, 647.

[56] H. Tom Diek, M. Svoboda, T. Z. Greiser, *Z. Naturforsch. B* **1981**, *36*, 823.

[57] R. Van Asselt, C. J. Elsevier, W. J. J. Smeets, A. L. Spek, R. Benedix, *Recl. Trav. Pays-Bas* **1994**, *113*, 88.

[58] M. Onishi, K. Igasawa, *Inorg. Chim. Acta* **1991**, *179*, 155.

[59] D. Mueller, G. Umbricht, B. Weber, A. Pfaltz, *Helv. Chim. Acta* **1991**, *74*, 232.

[60] I. Butula, G. Karlovic, *Justus Liebigs Ann. Chem.* **1976**, 1455.

[61] J. M. Kliegman, R. K. Barnes, *Tetrahedron* **1970**, *26*, 2555.

[62] G. R. Hoel, R. A. Stockland Jr., G. K. Anderson, F. T. Lapido, J. Braddock-Wilking, N. P. Rath, J. C. Mareque-Rivas, *Organometallics* **1998**, *17*, 1155.

[63] a) R. B. Schultz, *J. Organomet. Chem.* **1966**, *6*, 435; b) J. Chatt, L. M. Vallarino, L. M. Venanzi, *J. Chem. Soc.* **1957**, 3413.

[64] M. Brookhart, B. Grant, A. F. Volpe, *Organometallics* **1992**, *11*, 3920.

[65] *SADABS:* Area-Detector Absorption Correction; Siemens Industrial Automation, Inc.: Madison, WI, **1996**.

[66] A. Altomare, M. C. Burla, M. Camalli, G. Cascarano, C. Giacovazzo, A. Gagliardi, A. G. G. Moliterni, R. Spagna, *J. Appl. Crystallogr.* **1999**, *32*, 115.

[67] G. M. Sheldrick, SHELXL-97, A Program for Crystal Structure Refinement, University of Göttingen, Germany, 1997. Release 92-2.

[68] L. J. Farrugia, *J. Appl. Crystallogr.* **1999**, *32*, 837.